The chaperone FACT and histone H2B ubiquitination maintain S. pombe genome architecture through genic and subtelomeric functions

The chaperone FACT and histone H2B ubiquitination maintain *S. pombe* genome architecture through genic and subtelomeric functions

Magdalena Murawska[1], Tamas Schauer[2], Atsushi Matsuda[3, 4], Marcus D. Wilson[5], Thomas Pysik[1], Felix Wojcik[6], Tom W. Muir[6], Yasushi Hiraoka[3, 4], Tobias Straub[2], Andreas G. Ladurner[1, 7]

[1]Biomedical Center, Physiological Chemistry, Ludwig-Maximilians-University of Munich, 82152 Planegg-Martinsried, Germany

[2]Biomedical Center, Bioinformatics Unit, Ludwig-Maximilians-University of Munich, 82152 Planegg-Martinsried, Germany

[3]Advanced ICT Research Institute Kobe, National Institute of Information and Communications Technology, 588-2 Iwaoka, Iwaoka-cho, Nishi-ku, Kobe 651-2492, Japan

[4]Graduate School of Frontier Biosciences, Osaka University, 1-3 Yamadaoka, Suita 565-0871, Japan

[5]Wellcome Centre for Cell Biology, University of Edinburgh, Michael Swann Building, Kings Buildings, Mayfield Road, Edinburgh, EH9 3JR, UK

[6]Department of Chemistry, Princeton University, Princeton, NJ, 08544, USA

[7]Lead contact

Keywords: FACT, H2B ubiquitination, chromatin structure, histone chaperone, S. pombe

Correspondence: andreas.ladurner@bmc.med.lmu.de

SUMMARY

The histone chaperone FACT and histone H2B ubiquitination (H2Bub) facilitate RNA Polymerase II (RNAPII) passage through chromatin, yet it is not clear how they cooperate mechanistically. We used genomics, genetic, biochemical and microscopic approaches to dissect their interplay in *Schizosaccharomyces pombe*. We show that FACT and H2Bub globally repress antisense transcripts near the 5' end of genes and inside gene bodies, respectively. The accumulation of these transcripts is accompanied by changes at genic nucleosomes and RNAPII redistribution. H2Bub is required for FACT activity in genic regions. In the H2Bub mutant, FACT binding to chromatin is altered and its association with histones is stabilized, which leads to the reduction of genic nucleosomes. Interestingly, FACT depletion globally restores nucleosomes in the H2Bub mutant. Moreover, in the absence of Pob3, the FACT Spt16 subunit controls the 3' end of genes. Furthermore, FACT maintains nucleosomes in subtelomeric regions, which is crucial for their compaction.

INTRODUCTION

Eukaryotic DNA is packed into nucleosomes, which generally consist of 146 base pairs of DNA wrapped around an octamer of histone proteins (Karolin Luger, 1997; Larochelle et al., 2018). Nucleosomes help ensure the integrity of genome, but also constitute a major barrier for enzymes acting on DNA. Consequently, nucleosome assembly and the access of enzymes to DNA have to be firmly regulated. Histone chaperones are a diverse family of proteins that sequester histones from DNA and help deposit or remove them during DNA-based processes, including transcription, replication, and DNA repair (Hammond et al., 2017; Mattiroli et al., 2015; Nune et al., 2019; Warren and Shechter, 2017).

FACT (Facilitates Chromatin Transcription) is an essential histone chaperone that is highly conserved from yeast to humans and is composed of two subunits, Spt16 and SSRP1/Pob3 (Gurova et al., 2018). Spt16 was first identified as a suppressor of Ty elements in *S. cerevisiae*, while Pob3 was identified by co-purification with DNA polymerase I (Clark-Adams and Winston, 1987; Wittmeyer and Formosa, 1997). The human FACT complex was identified as a factor essential for RNA Polymerase II to transcribe through chromatin (Orphanides et al., 1998; Winkler et al., 2011). Several domains of the two subunits of FACT are involved in binding core histones. In particular, H2A-H2B dimers are bound by the unstructured C-terminal domains of Spt16 and Pob3 which compete with DNA binding to histones (Hondele et al., 2013; Kemble et al., 2015). FACT is predominantly associated with gene bodies of actively transcribed genes *in vivo* (Duina et al., 2007; Lee et al., 2017; Mayer et al., 2010).

FACT is overexpressed in various tumors and stem cells, suggesting a role in the maintenance of undifferentiated cell states (Garcia et al., 2011) and has been

implicated in genome stability (Herrera-Moyano et al., 2014) and chromosome segregation (Lejeune et al., 2007).

Despite recent progress in our understanding of FACT function, it is still not understood how and which genic nucleosomes FACT recognizes, and how its activity is modulated in distinct genomic contexts. Further, whether and how the two subunits of FACT have distinct functions has not been well studied in a genome-wide context.

One histone modification suggested to cooperate with FACT during transcription elongation is the monoubiquitination of H2B (H2Bub) (Hartzog and Quan, 2008; Pavri et al., 2006). Pioneering research has shown that H2Bub together with FACT stimulates transcription *in vitro* on a chromatinized template (Pavri et al., 2006). H2Bub is important for nucleosome reassembly after the passage of RNAPII in *S. cerevisiae* (Batta et al., 2011; Fleming et al., 2008; Lee et al., 2012). In some chromatin contexts H2Bub contributes to FACT binding or stabilization at chromatin (Fleming et al., 2008; Trujillo and Osley, 2012). Further, a recent report showed that FACT stimulates deubiquitinase activity of Ubp10 in *S. cerevisiae* (Nune et al., 2019), adding an additional layer of complexity to the interplay between FACT and H2Bub. However, it is still not clear how and to which extent FACT and H2Bub cooperate in gene transcription and nucleosomal transactions (Nune et al., 2019). Moreover, there are contradicting results on the effects of H2Bub on mononucleosome stability *in vitro*, nucleosome fiber decompaction *in vitro*, and its functions *in vivo* (Batta et al., 2011; Chandrasekharan et al., 2009; Debelouchina et al., 2016; Segala et al., 2016). Whether H2Bub has a direct role in FACT binding or chaperoning activity, is not known.

We used the fission yeast *Schizosaccharomyces pombe* as a powerful model organism to study FACT and H2Bub functions in genome organization. One of the convenient features of *S. pombe* is that deletion of the *pob3* gene reduces FACT

activity without causing lethality as in *S. cerevisiae* or other model organisms (Lejeune et al., 2007). We applied genomics, genetics, biochemistry and high-resolution microscopy to comprehensively dissect the relationship between FACT and H2Bub in *S. pombe*. Our results show that within gene bodies, FACT and H2Bub contribute to the proper maintenance of genic nucleosomes and repression of antisense transcription at 5' and gene bodies, respectively. Analysis of the double mutant supported by *in vitro* assays revealed mechanisms by which FACT and H2Bub cooperate at gene bodies. Finally, we show that FACT and H2Bub regulate highly compacted knob structures at subtelomeres. In particular, FACT together with Set2/H3K36me pathway is important for subtelomere compaction. Altogether, our results provide novel insights into FACT and H2Bub cooperativity in the gene bodies and suggest a role of FACT in the maintenance of higher order chromatin structure outside of euchromatin.

RESULTS

H2Bub or FACT loss leads to global de-repression of antisense transcription

To address the potential cooperativity between FACT and H2Bub in gene regulation, we first compared the effects on gene expression in *H2BK119R* and *pob3Δ* strains, in which H2Bub is missing and FACT function is impaired, respectively. We performed strand-specific RNA-seq in two highly reproducible biological replicates (Figure S1A). Both H2Bub and FACT affect gene activity (Figure 1A and B). There were 994 genes significantly up-regulated and 1001 genes down-regulated in the FACT mutant and 1418 and 1374 genes up- and down-regulated in the *H2BK119R* mutant, respectively (Figure S1B). Despite the similar number of the misregulated genes in both mutants, the correlation between them was relatively low (Figure S2A), suggesting that FACT and H2Bub regulated genes overlap only partially. Strikingly, both mutants exhibit a global effect on the de-repression of antisense transcription

(Figure 1A and 1B). There were 2012 antisense transcripts significantly up-regulated in the *H2BK119R* mutant and 2450 in the *pob3Δ* mutant (Figure S1B). There was also a positive correlation between antisense transcripts de-repressed in both strains (Figure S2B) suggesting a significant overlap between antisense transcripts repressed by FACT and H2Bub. Thus, FACT and H2Bub globally repress antisense transcription in *S. pombe*.

H2Bub and FACT repress antisense transcription distinctly

To investigate whether the de-repressed antisense transcripts effect the corresponding sense transcription, we clustered the genes based on the relationship between sense and antisense transcription (Figure 1C). Many genes with increased antisense RNAs were slightly down-regulated in both strains (Figure 1C, cluster I). On the other hand, a similar number of genes were up-regulated, while the antisense RNAs were also de-repressed (Figure 1C, cluster II). The cluster with down-regulated genes and antisense transcripts was relatively small (Figure 1C, cluster III). The same applies to the cluster with up-regulated genes and down-regulated antisense transcripts (Figure 1C, cluster IV). Thus, a large number of genes might be potentially down-regulated due to increased antisense transcription in both *H2BK119R* and *pob3Δ* mutants. However, a similar number of genes are up-regulated, despite having similarly de-repressed antisense transcription. This analysis is in accordance with the scatterplots, which did not reveal any correlation between sense and antisense transcripts (Figure 1A and 1B).

Interestingly, the heatmaps suggested specific patterns of antisense transcripts in the FACT and H2Bub mutants (Figure 1C). In order to compare those patterns, we scaled the genes and aligned them to the transcription start site (TSS) and transcription termination site (TTS; Figure S1C). This analysis revealed that the distribution of the antisense transcripts repressed by H2Bub and FACT is distinct

(Figure S1C). The metaplot of antisense RNA (Figure 1D) shows that antisense transcripts accumulate in the gene bodies of the H2Bub mutant and decline towards the 5' end of genes. In contrast, in the FACT mutant, the antisense transcripts slowly increase towards the 5' end of genes and terminate shortly upstream of TSS (Figure 1D).

Since both FACT and H2Bub are associated with transcription elongation, we monitored elongating RNAPIISer2P distribution by ChIP-seq in both mutants. We divided the genes based on their expression levels in the *wt* strain and plotted log2 Fold Change (log2FC) of RNAPIISer2P ChIP-seq signal between the mutant and the *wt* strain (Figure 1E). RNAPIISer2P in the *H2BK119R* mutant is reduced at highest expressed genes and it shows a distinct peak downstream of TTS at all genes (Figure 1E). The 3' end shift of RNAPII in this strain was reported previously (Sanso et al., 2012) and it might be related to the role of RNAPIISer2P in 3' end processing and transcription termination (Larochelle et al., 2018). Thus, in addition to repression of genic antisense transcription, H2Bub has likely functions related to transcription termination in *S. pombe*. In the *pob3Δ* mutant, RNAPIISer2P signal increases around 5' end of genes which correlates with the increase of antisense transcription in this strain (Figure 1D and 1E).

Together, our results suggest that FACT and H2Bub preferentially repress antisense transcripts associated with specific gene regions: TSS and 5' end or the gene bodies, respectively.

Loss of H2B ubiquitination or FACT function alters genic nucleosomes in a distinct manner

Our findings suggest that FACT and H2Bub protect different parts of genes against cryptic antisense transcription. We hypothesized that H2Bub controls nucleosomes over gene bodies, while FACT controls nucleosomes more proximal to the TSSs. To test this, we mapped nucleosomes in the FACT and H2Bub mutants by micrococcal

nuclease digestion of chromatin and deep sequencing of the protected DNA (MNase-seq). To get a better molecular range of the assay and to avoid over-digestion by MNase, we used four different concentrations of MNase (Figure S3A), similar to a method previously reported (Mieczkowski et al., 2016).

First, our analysis shows that distinct nucleosomes in the wild-type strain have a different sensitivity to the MNase treatment (Figure S3B). The +1 and the -1 nucleosomes and the upstream intergenic nucleosomes are most sensitive to the digestion, while the nucleosomes starting from the +2 position are relatively resistant to the degree of the MNase treatment (Figure S3B).

Next, we determined genic nucleosome changes in the H2Bub and FACT mutants. We analyzed the samples treated with the lowest MNase concentration, where the +1 nucleosome was most intact (Figure S3B). Metaplots of the genic nucleosomes centered at the TSS +1 or at the TTS -1 nucleosome show global defects in nucleosomal arrays over gene bodies in both strains (Figure 2A and 2B). In the *H2BK119R* mutant, the +1 and the TSS proximal nucleosomes are better protected, while the nucleosomes starting from the +2 position progressively lose occupancy (Figure 2A). Additionally, we performed H3 ChIP-seq in the *H2BK119R* mutant which did not show a reduction of histone signal in the gene bodies, which suggests that the increased sensitivity of the genic nucleosomes to the MNase treatment in the absence of H2Bub reflects less stable or improper assembled nucleosomes, rather than a histone loss (Figure 2C). This impairment of genic nucleosomes is in agreement with the function of H2Bub in the assembly of genic nucleosomes during transcription elongation (Batta et al., 2011). The protection of the +1 nucleosome in the *H2BK119R* strain has not been reported before and it could explain why the antisense transcripts around the TSS in the H2Bub mutant are not increased (Figure 1D).

In contrast to previous observations in *S. cerevisiae* (True et al., 2016), our characterization of the *pob3Δ* mutant revealed only a minor global decrease of

nucleosomes in gene bodies by MNase-seq and H3 ChIP-seq (Figure 2B and 2C). We observed a general defect at +1 and TSS proximal nucleosomes, which appear to have lower peaks (Figure 2B). In addition, the genic nucleosomes starting from the +2 nucleosome are shifted in the *pob3Δ* mutant and the amplitudes of the regions between the nucleosomes are lower. This indicates a problem with nucleosome phasing and possibly nucleosome positioning in the FACT mutant (Figure 2B and S3C middle and right panel). Under higher MNase digestion, the density of genic nucleosomes in the FACT mutant is reduced (Figure S3A). Together with the subtle changes showed by H3 ChIP-seq, our results indicate the presence of less stable nucleosomes in the *pob3Δ* strain, rather than overall nucleosome loss.

To determine whether changes on the metaplots reflect global changes or only changes in a limited group of genes, we generated heatmaps of fold changes in the nucleosome dyad densities with all the protein coding genes in which we could call the +1 nucleosome in both *H2BK119R* and *pob3Δ* strains. We ordered the heatmaps according to the transcription clusters as in Figure 1C. This confirmed, that the changes in the genic nucleosomes are global and they occur at the majority of protein coding genes (Figure 2D). Thus, both FACT and H2Bub globally control genic nucleosomes in *S. pombe* in a distinct manner.

The increased MNase sensitivity of the +1 nucleosome in the FACT mutant might be related to the presence of the H2A.Z variant. FACT cannot deposit this histone variant into nucleosomes in budding yeast and H2A.Z gets incorporated to ectopic sites of the genome in a FACT mutant (Heo et al., 2008; Jeronimo et al., 2015). We selected genes with or without H2A.Z peaks from the published ChIP-seq dataset (Nissen et al., 2017) and compared their nucleosomal arrays in both mutants. We observed better positioned nucleosomes upstream of the TSS on genes with the H2A.Z variant in the wild-type strain (Figure S3D), as previously published (Guillemette et al., 2005). However, there is a very similar decrease of the +1

nucleosome in the *pob3Δ* strain in both gene classes (Figure S3D). The same applies to the *H2BK119R* mutant, in which the +1 nucleosome is better protected at both classes of the genes. Thus, the +1 nucleosome occupancy changes present in the FACT and H2Bub mutants are independent of the presence of H2A.Z.

FACT inactivation suppresses H2Bub mutant nucleosome and transcription phenotypes

Our analysis in the single H2Bub and FACT mutants indicates that FACT and H2Bub protect from cryptic antisense transcription by acting at different gene regions. To test the functional relationship between these two factors, we repeated our experiments in the *pob3ΔH2BK119R* double mutant. Surprisingly, we observed that the double mutant produces phenotypes that strongly resemble the phenotype of the single FACT mutant (Figure 3, S2 and S4). First, an inspection of the nucleosomes in the genome browser revealed that the decreased genic nucleosomes in the *H2BK119R* mutant are often restored in the double mutant (Figure 3A). Second, the metaplot of the density of genic nucleosomes clearly show a global restoration of genic nucleosomes in the double *pob3ΔH2BK119R* mutant (Figure 3B, 3E, S4B and S4C). Finally, the antisense transcription profile mirrors the profile of the single mutant (Figure 3C and S4A). Interestingly, *pob3Δ* suppresses also RNAPII loss at highly expressed genes in the *H2BK119R* strain but it does not suppress the 3' end shift of RNAPII downstream of TTS, suggesting that the 3' end function of H2Bub is unrelated to FACT (Figure 3D). These data show that FACT inactivation in the H2Bub mutant suppresses both the nucleosome reduction and genic antisense transcription observed in the single *H2BK119R* mutant. This result clearly demonstrates that *pob3Δ* is epistatic to *H2BK119R* in gene bodies.

H2B ubiquitination limits FACT association to gene bodies and facilitates histone deposition onto DNA by FACT

The unexpected suppression of the *H2BK119R* mutant phenotypes by FACT depletion suggests that in the absence of H2Bub, FACT activity is altered. We hypothesized that H2Bub may regulate directly the binding of FACT to chromatin, its association with histones and/or the chaperoning activity. To test it, we performed ChIP-seq of two FACT subunits (Spt16 and Pob3) in the *H2BK119R* strain. The log2FC profiles of FACT binding revealed a decrease of FACT from 5' gene ends at highest expressed genes and a global shift of FACT downstream of TTS at all genes (Figure 4A). Strikingly, those profiles resemble RNAPIISer2P profile in the *H2BK119R* strain (Figure 1E), suggesting that FACT might be more directly associated with elongating RNAPII.

Next, we immunoprecipitated endogenous Flag-tagged histone H2B from *wt* or *H2BK119R* strains and checked for the association of FACT by western blot (Figure 4B). Surprisingly, we reproducibly observed around 1.5 - fold more FACT complex associated with the bulk of non-ubiquitinated histones compared to a bulk of wild-type histones (Figure 4C). Importantly, FACT total protein levels are not much changed in this mutant (Input in Figure 4B). This result suggests that loss of H2B ubiquitination may stabilize FACT association with histones *in vivo*. To check if this is a direct effect, we performed *in vitro* EMSA experiment where recombinant FACT was incubated with increasing amounts of unmodified or ubiquitinated histone dimers (Figure 4D). This experiment revealed a small but reproducible reduction of around 20% of the binding affinity of FACT to H2A-H2B dimers in the presence of ubiquitination (Figure 4E). Thus, H2Bub reduces FACT binding to histones both *in vivo* and *in vitro*.

To check whether FACT chaperone activity is affected by H2Bub, we performed nucleosome chaperoning assays with recombinant FACT and recombinant histone octamers (Figure 4F). We pre-incubated FACT with unmodified or ubiquitinated

histone octamers (Figure S5B and S5D) (McGinty et al., 2009). Next, we added DNA bearing the Widom 601 positioning sequence in a suboptimal concentration. Under these conditions, histones and DNA precipitate and do not enter the gel. Only when a histone chaperone is present, the chaperone will bind the histones and promote their deposition onto DNA, thus restoring nucleosomes. We monitored the assembled products on a native acrylamide gel (Figure 4G). In the presence of FACT, we reproducibly observe a higher recovery of ubiquitinated assembly species in comparison to the unmodified ones (Figure 4G and 4H). Importantly, the ubiquitinated octamers assemble with similar efficiency as wild-type during salt gradient assembly (Figure S5E). This result suggests that H2Bub enhances histone deposition onto DNA by FACT.

Together, our ChIP-seq, Co-IP, *in vitro* binding experiments and the assembly assay indicate that H2Bub is important to maintain proper association of FACT within gene bodies and proper assembly activity of FACT. We postulate that H2Bub fine-tunes the chaperone-histone binding dynamics which facilitates the deposition of histones onto DNA during the assembly reaction. These results also explain why FACT inactivation suppresses the nucleosome phenotype in the *H2BK119R* strain. In the absence of H2Bub, FACT binding to histones is stabilized and histone deposition by FACT is likely weaker. This would lead to the “sequestration” of both FACT and histones and the subsequent destabilization of genic nucleosomes. We propose that upon FACT depletion the FACT “trapped” histones get released and the genic nucleosomes are reassembled in the *pob3∆H2BK119R* double mutant.

The Pob3 subunit of FACT regulates the 5’ end of genes

The different effects of FACT and H2Bub within the 5’-end of genes and gene bodies raise the question how their genic functions are separated. Both H2Bub and FACT are associated with active genes (Duina et al., 2007; Lee et al., 2017; Mayer et al., 2010; Van Oss et al., 2016). We mapped H2Bub and FACT subunits in *S. pombe* by

ChIP-seq. As expected, both factors are strongly enriched on highly expressed genes and weaker with low expressed genes (Figure 5A and 5B). We generated metaplots of H2Bub and FACT subunits on highly expressed genes and aligned them to the +1 and -1 nucleosomes (Figure 5A). The data clearly show that H2Bub signal increases at TSS and decreases at TTS. FACT signal is slightly shifted downstream of H2Bub in relation to the +1 nucleosome. Surprisingly, FACT signal continues two nucleosomes downstream of TTS. This extended association of FACT downstream of TTS resembles RNAPIISer2P association with gene bodies (Figure 5A). Thus, the genic profiles of FACT and H2Bub suggest a different order of recruitment and dissociation from gene bodies but they do not explain the specific 5' gene changes in the *pob3Δ* mutant.

The fact that *spt16* but not *pob3* deletion is lethal in *S. pombe* suggests that Spt16 may have separate functions in this organism. To address this possibility, we performed ChIP-seq of Spt16 in the *pob3Δ* mutant. Despite Spt16 protein levels are reduced in the absence of Pob3, we were surprised to detect a significant amount of Spt16 bound to the genes in the *pob3Δ* background (Figure 5B). Moreover, Spt16 association with genes is altered in the absence of Pob3. On highly expressed genes Spt16 is strongly depleted from 5' of the genes, while on low and moderately expressed genes Sp16 accumulates towards 3' of the genes (Figure 5B and 5C). Next, we plotted log2FC of RNAPIISer2P signals, antisense transcription and nucleosomal changes on highly or low/moderately expressed genes in the *pob3Δ* mutant and we compared them with the changes of Spt16 signals (Figure 5C). The presence of Spt16 at 3' of the genes correlates with reduction of antisense transcription, reduced increase of RNAPII signals and nucleosomal "fuzziness" (Figure 5C). Together, our results suggest that Pob3 has specific functions at the 5' end of genes to repress antisense transcription and assure proper nucleosome assembly. Pob3 is also important for correct association of Spt16 within gene bodies.

We suggest that the remaining Spt16 subunit bound to 3' gene ends at both highly and low expressed genes likely maintains FACT functions in the absence of Pob3. In this context, Spt16 protects those parts of the genes from aberrant antisense transcription.

Loss of FACT changes subtelomeric gene expression and knob formation

Subtelomeres are enriched for meiotic and stress-response genes in *S. pombe* (Mata et al., 2002) (Figure 6A). Chromatin perturbation in this region may lead to changes in transcription of the subtelomeric genes. We checked whether FACT and H2Bub have an effect on the transcription of these genes. RNA-seq analysis along chromosomal coordinates revealed increased transcription at both ends of chromosome I and the right arm of chromosome II in the FACT mutant (Figure 6B, 6C, S6A, S6B and S6C).

Next, we analyzed the nucleosome density at subtelomeres and compared them to the rest of the genome (Figure 6D). The overall subtelomeric nucleosome density is significantly decreased in the *pob3Δ* mutant (Figure 6D, S6B and S6C). Thus, the nucleosome changes in *pob3Δ* strain correlate with the transcription changes of the subtelomeric genes. Interestingly, the *H2BK119R* mutant has a small but significant increase of the nucleosome density at subtelomeres, while the double mutant has a phenotype similar to *pob3Δ* in both transcription and nucleosome density at subtelomeres (Figure 6C, 6D, S6B and S6C).

Subtelomeres in *S. pombe* are characterized by a presence of a specific chromatin domain, depleted of H3K9me and active histone marks (Buchanan et al., 2009; Matsuda et al., 2015). In addition, those regions are strongly compacted into so-called 'knobs' (Matsuda et al., 2015). Our results suggest that knobs could be affected in the FACT mutant. Thus, we counted knobs in our mutant strains and

found that there is a 50% decrease of knobs in the *pob3Δ* mutant and in two conditional *spt16* ts alleles (Figure 6E and S6E). Unexpectedly, in the *H2BK119R* mutant, almost 100% of cells have 1 or 2 knobs and this phenotype is reversed to the *wt* knob number in the double *pob3ΔH2BK119R* mutant (Figure 6E). Next, we checked if H2Bub is present at knobs. We performed high-resolution microscopy on the nuclei stained with H2Bub specific antibody. There is a clear co-localization of H2Bub mark with knobs suggesting that H2Bub in contrast to other active histone marks is not depleted from knobs (Figure S6D). In addition, ChIP-seq with H2Bub antibody showed discrete peaks of H2Bub at subtelomeric regions (Figure S6F). Our results suggest that H2Bub might be directly involved in knob decompaction. FACT depletion likely removes the nucleosome barrier and restores knobs to *wt* level in the absence of H2Bub.

Next, we investigated the pathway through which FACT maintains knobs. Set2 and H3K36me are important for knob regulation (Matsuda et al., 2015). As *set2Δ* has very little knobs, we used *H3K36R* mutant background to be able to observe synthetic interactions. In the *H3K36R* mutant there is around 20% reduction of knobs as in comparison to the corresponding *wt* strain (Figure 6F). In the same genetic background in the *pob3Δ* mutant there is 50% reduction of knobs (Figure 6F). The double *pob3ΔH3K36R* mutant behaves the same as the *pob3Δ* mutant clearly showing that FACT works in the same pathway as Set2/H3K36me to maintain knobs.

Overall our results indicate that FACT contributes to nucleosome maintenance at subtelomeres in *S. pombe* through Set2/H3K36me pathway. Our analysis also indicates that FACT and H2Bub have opposite effects on knob maintenance and that their functions depend on the genomic context.

DISCUSSION

By integrating genomics, genetic, biochemical and microscopic approaches, we have comprehensively dissected the relationship between FACT and H2Bub and their functions in chromatin integrity. We show that by impairing FACT or H2Bub in *S. pombe*, different classes of genic antisense RNAs are de-repressed globally. Pob3 subunit of FACT controls antisense transcripts enriched towards the 5' ends of genes, while H2Bub represses antisense transcription within gene bodies (Figure 7). Transcriptional alterations correlate with nucleosome density changes in the *pob3Δ* and *H2BK119R* mutants (Figure 7). Our data underpin the mechanisms by which FACT and H2Bub control different regions of a gene in fission yeast.

Despite several previous studies, it has not been clear how FACT and H2Bub cooperate during transcription. It has been suggested that H2Bub helps FACT to displace H2A-H2B dimer and thus stimulates *in vitro* transcription on a chromatinized template (Pavri et al., 2006). In addition, H2Bub might stabilize FACT association with chromatin in *S. cerevisiae* (Fleming et al., 2008; Trujillo and Osley, 2012). Here we show that in accordance with previous reports in budding yeast and in higher eukaryotes (Batta et al., 2011; Kolundzic et al., 2018; True et al., 2016), a similar number of genes are misregulated in H2Bub and FACT mutants. Additionally, there is a global up-regulation of specific genic antisense transcripts in both mutants. FACT predominantly represses antisense transcripts enriched near 5' proximal regions of the coding genes. The observed 5' antisense transcription in the *pob3Δ* mutant correlates with an increased signal for RNAPII Ser2P and decreased occupancy of the +1 nucleosome in this strain. Unexpectedly, we find that the Spt16 subunit of FACT is still associated with genes in the absence of Pob3. However, its localization is altered. Spt16 is depleted from the 5' end of genes, but not the 3' end of highly expressed genes and it accumulates towards the 3' end at low and moderately expressed genes. Our results suggest that 3'-end associated Spt16 maintains some of the FACT activity and protects 3' gene ends from antisense

transcription. Previously, SSRP1 was shown to have Spt16-independent roles in transcription of only a small subset of genes and in DNA repair (Dinant et al., 2013; Li et al., 2007). Intriguingly, our results reveal a separation of functions for the two FACT subunits within gene bodies on a genome-wide scale. Our observations likely establish a rationale for the fact that the deletion of *pob3* in *S. pombe* is not lethal.

RNAPII transcribing the antisense strand in the *pob3Δ* mutant may lead to the instability of the +1 nucleosome. Indeed, it was suggested that the ongoing cryptic transcription in the *spt16* mutant leads to histone loss in *S. cerevisiae* (Feng et al., 2016). Our results cannot exclude the possibility that the +1 nucleosome has an antisense barrier function (McCullough et al., 2019) and that FACT is important for the establishment of this barrier.

We find that the H2Bub mutant accumulates antisense transcripts evenly distributed across the gene bodies, which terminate before the TSS. The different pattern of antisense transcription towards the 5' end of genes in the *H2BK119* mutant is likely associated with the effect of H2Bub on the +1 nucleosome. In the H2Bub mutant, the TSS proximal nucleosomes are better protected against MNase digestion. Our data suggest a role for H2Bub in the disassembly of the TSS proximal nucleosomes.

Furthermore, we demonstrated that H2Bub plays several roles in FACT regulation. First, in the absence of H2Bub, FACT is redistributed downstream of TTS. Strikingly, FACT chromatin association changes in the *H2BK119R* mutant resemble RNAPIISer2P alterations in this strain. This suggests that FACT association with genes might be partially dependent on elongating RNAPII. Second, we propose that H2Bub increases histone-chaperone dynamics, which in turn is important to facilitate histone deposition on DNA and subsequent nucleosome assembly. Several observations support our hypothesis. Co-IPs from cell extracts show more FACT associated with H2B in the *H2BK119R* mutant. Further, EMSAs with recombinant proteins show a decrease of binding affinity of FACT to ubiquitinated dimers. In

addition, more assembly products are recovered in the chaperone assay in the presence of H2Bub. Furthermore, deletion of *pob3* suppresses nucleosome occupancy and genic antisense transcription in the *H2BK119R* mutant likely through a release of FACT-bound histones.

How can H2Bub reduce FACT binding to H2A-H2B dimers? One possibility is that ubiquitin masks certain FACT binding epitopes on histones and thus reduces its binding. The acidic patch residues are important for the activity of chromatin remodelers and for FACT binding to histones (Dann et al., 2017; Hodges et al., 2017). A recent cryo-EM structure of CHD1 with ubiquitinated nucleosome revealed that ubiquitin may regulate access to the nucleosomal acidic patch (Sundaramoorthy et al., 2018). Thus, by blocking access to the acidic patch, H2Bub could decrease the affinity of FACT for histones. Future work will establish the exact molecular mechanism of H2Bub on the FACT activity.

Additionally, our results indicate that FACT might control higher order structure of subtelomeric knobs. First, the subtelomeric genes are up-regulated in the FACT mutant. Second, there is a reduction of the nucleosome density in subtelomeric regions in the *pob3Δ* strain and finally, knobs are impaired to around 50% in the FACT mutants. Our genetic analysis shows that FACT works together with H3K36 methylation pathway to maintain knobs. The Set2/H3K36me3 pathway is important for knob formation, transcriptional silencing of subtelomeres and post-transcriptional silencing of heterochromatin in *S. pombe* (Matsuda et al., 2015; Suzuki et al., 2016). Our results suggest that FACT and H3K36me likely affect nucleosome assembly or the stability of nucleosomes at subtelomeric regions. Correctly assembled nucleosomes might be important for binding of other factors, which in turn assure proper knob compaction. In line with this, histone H2A phosphorylation is crucial for the recruitment of shugoshin, a protein essential for knob organization (Tashiro et al., 2016).

The persistent presence of knobs in the *H2BK119R* mutant is less clear. H2Bub was shown to protect euchromatin from uncontrolled spreading of heterochromatin (Flury et al., 2017). It is possible that in the absence of H2Bub, subtelomeric heterochromatin spreads into knobs affecting their decompaction. However, we did not observe subtelomeric heterochromatin spreading in the *H2BK119R* strain (Figure S6F). Several lines of evidence argue that H2Bub might be directly involved in knob decompaction. First, H2Bub is not excluded from knobs as other active histone marks. Second, subtelomeric nucleosomes are better protected from MNase digest in the *H2BK119R* strain. Finally, deletion of *pob3,* which reduces subtelomeric nucleosomes, restores knob number to the wild-type levels in the H2Bub mutant. Together, we suggest that H2Bub is important for knob decompaction in *S. pombe*. This would be in line with the role of H2Bub in the decompaction of nucleosomal arrays *in vitro* (Debelouchina et al., 2016).

In conclusion, our work discovered novel and genome context-specific relationships between FACT and H2Bub in *S. pombe*. The effects of FACT on nucleosome maintenance and knob formation allows us to speculate that FACT might help to safeguard specific chromatin states outside of canonical euchromatin domains. As both H2Bub and FACT functions are misregulated in human cancers, it will also be interesting to investigate how our results might be applicable to cancer cells.

ACKNOWLEDGMENTS

This research was supported by the European Commission (Marie-Curie Individual Fellowship H2020-MSCA-IF-2014 contract 657244 to M.M.) and the Friedrich-Baur-Stiftung to M.M., DFG SFB1064 and DFG SFB1309 collaborative research centers to A.G.L., Z04/SFB1064 to T. St. and T. Sc., NIH Grants R37 GM086868, R01 GM107047 and P01 CA196539 to T.W.M.; JSPS KAKENHI JP19H03202 to A.M. F.W. was funded by a postdoctoral fellowship from DFG (WO 2039/1-1). M.D.W. is

supported by the Wellcome Trust [210493] and University of Edinburgh. The Wellcome Centre for Cell Biology is supported by core funding from the Wellcome Trust [203149]. We thank Alexander Brehm and Fred Winston for insightful comments on the manuscript and Carla Margulies for advice. We thank Sigurd Braun, Philipp Korber and Silke Krause for sharing protocols and Julia Preißer for help with cell culture. We thank LAFUGA and Stefan Krebs and Helmut Blum for sequencing.

AUTHOR CONTRIBUTIONS

Conceptualization, M.M. and A.G.L.; Investigation, M.M., A.M., T.P.; Formal Analysis, T.Sc. and T.St.; Visualization, M.M., T.Sc., A.M., T.P.; Resources, M.D.W., F.W., T.W.M.; Writing - Original Draft, M.M. and A.G.L.; Writing - Review and Editing, M.M. and A.G.L.; Funding acquisition, M.M. and A.G.L.; Supervision, A.G.L., T.St., Y.H.

DECLARATION OF INTERESTS

The authors declare a competing interest. Andreas Ladurner is Co-Founder and CSO of Eisbach Bio GmbH.

MAIN FIGURE TITLES AND LEGENDS

Figure 1. Loss of H2B ubiquitylation or loss of FACT subunit *pob3* leads to global increase of anti-sense transcription at gene bodies or at TSS proximal regions, respectively.

A) Density colored scatterplots comparing RNA-seq log2 Fold Change (log2FC) of sense (x-axis) and antisense (y-axis) transcripts between *H2BK119R* and wild-type (WT) strains or B) between *pob3Δ* and wild-type (WT) strains. Quadrants are labeled by roman numbers (I: sense < 0 – antisense > 0; II: sense > 0 – antisense > 0; III: sense < 0 – antisense < 0, IV: sense > 0 – antisense < 0). All protein coding genes are considered (total = 5069). Average of 2 biological replicates is shown.

C) Heatmaps of RNA-seq log2FC aligned to transcription start (TSS). Left: *H2BK119R* vs. wild-type (WT) (sense and antisense) and right: *pob3Δ* vs. wild-type (WT) (sense and antisense). Heatmaps include genomic regions 1 kb upstream and 5 kb downstream to TSS. Genes are ordered by length and grouped based on in which quadrant (I-IV) they are in 1A or 1B, respectively (total = 5069).

D) Metaplots of RNA-seq log2FC aligned and scaled to transcription start (TSS) and termination sites (TTS). Left panel: sense; right panel: antisense. Colors: orange – *H2BK119R* vs. wild-type (WT); blue – *pob3Δ* vs. wild-type (WT). The plot represents the same genes as in C.

E) Metaplots of log2FC between mutant vs. wild-type of RNAPIISer2P ChIP-seq aligned and scaled to TSS and TTS. Genes were divided into 4 quantiles based on their expression level in the *wt* strain. The darker the color shade, the higher expression level. Colors: orange – *H2BK119R* vs. wild-type (WT); blue – *pob3Δ* vs. wild-type (WT). Average of 2 biological replicates is shown.

Figure 2. Loss of H2B ubiquitylation or loss of *pob3* alters nucleosome structure in a different manner.

A-B) Metaplots of normalized nucleosome density (MNase-seq) centered at the TSS +1 nucleosome (left) or at the TTS -1 nucleosome (right). The plots include a +/- 1 kb region surrounding the center. Gene body nucleosome positions are marked with dashed vertical lines. Colors: grey – wild-type (WT); orange – *H2BK119R*; blue – *pob3Δ*. Protein coding genes with called TSS +1 nucleosome (total = 4524) or with TTS -1 nucleosome (total = 3794) are considered. Nucleosomes were called in the wild-type strain. Average of 2 biological replicates is shown.

C) Metaplots of log2FC between mutant vs. wild-type of H3 ChIP-seq centered at the TSS +1 nucleosome (left) or at the TTS -1 nucleosome (right). Genes were divided into 4 quantiles based on their expression level in the *wt* strain. The darker the color shade, the higher expression level. Colors: orange – *H2BK119R* vs. wild-type (WT); blue – *pob3*D vs. wild-type (WT).

D) Heatmaps of Fold Change between mutant vs. wild-type nucleosome density centered at the TSS +1 nucleosome. Left: *H2BK119R* vs. wild-type (WT) and right: *pob3Δ* vs. wild-type (WT). The plots represent the same genes as in A-B, and genes are grouped (I-IV) by RNA-seq the same way as in Figure 1A-C. Gene body nucleosome positions are marked with dashed vertical lines.

Figure 3. FACT deletion suppresses nucleosome and transcription defects of the H2Bub mutant at genic regions.

A) Example regions of nucleosome density on chromosome I (left) and on chromosome II (right). Colors: grey – wild-type (WT); orange – *H2BK119R*; blue – *pob3Δ*; magenta – *pob3Δ H2BK119R*. Two biological replicates are shown.

B) Metaplot of nucleosome density (MNase-seq) centered at the TSS +1 nucleosome. The plot includes a +/- 1 kb region surrounding the center. Gene body nucleosome positions are marked with dashed vertical lines. Average of 2 biological replicates is shown. Colors: same as in A).

C) Metaplot of RNA-seq antisense log2 Fold Change between mutant vs. wild-type aligned and scaled to TSS and TTS. Colors: same as in B.

D) Metaplots of log2FC between *pob3ΔH2BK119R* vs. wild-type (WT) of RNAPIISer2P and E) H3 ChIP-seq aligned and scaled to TSS and TTS. Genes were divided into 4 quantiles based on their expression level in the *wt* strain. The darker the color shade, the higher expression level.

Figure 4. H2Bub reduces FACT binding to histones *in vivo* and facilitates histone deposition on DNA by FACT *in vitro*.

A) Metaplots of log2FC between *H2BK119R* vs. wild-type (WT) of Pob3 and Spt16 ChIP-seq aligned and scaled to TSS and TTS. Genes were divided into 4 quantiles based on their expression level in the *wt* strain. The darker the color shade, the higher expression level. Average of 2 biological replicates is shown.

B) Benzonase treated WCE from the wild-type or *H2BK119R* strains were immunoprecipitated to pulldown Flag-tagged H2B. IPs were washed with the indicated salt concentrations. Association of FACT subunits with the Flag-H2B or Flag-H2BK119R was monitored by western blot. Input represents 10% of the initial material.

C) Quantification of FACT association with the wild-type or H2BK119R histone. The experiment was performed as in Figure 4B with the difference that washes were done in 250 mM NaCl. The associated FACT signal was normalized to the immunoprecipitated histone signal and normalized to 1 for the wild-type strain. The average of 3 - 4 independent experiments is shown, error bars represent SEM, p values (two-tailed Student's t test) are shown.

D) EMSA of FACT and histone dimer binding. Recombinant FACT (0.8 μM) was incubated with increasing amounts of H2A-H2B or H2A-H2Bub dimers. The products

were resolved on the 5.5% native PAA gel and stained with Coomassie Blue. A representative gel is shown.

E) Quantification of 3 independent EMSA experiments. Error bars represent SDEV, apparent Kd is shown in nM.

F) Schematic of the histone chaperoning assay.

G) Histone chaperoning assay. 46.3 nM of wild type or ubiquitinated histone octamers were pre-incubated with 150 nM of FACT as indicated. 11.2 nM of Cy3 labeled 601 DNA fragment was added to the histone-FACT complexes and further incubated for 30 min at 37°C. The samples were spun-down and the supernatants were resolved on the 6% native PAA gel. Gel was scanned with Typhoon FLA9500. The positions of free DNA and assembly products are indicated on the right. A representative gel is shown.

H) Quantification of the recovered products from chaperoning assays performed as in Figure 4G. The quantification represents average from 3 independent experiments, error bars indicate SDEV, p value (two-tailed Student's t test) is shown.

Figure 5. Pob3 subunit of FACT regulates 5' of the genes

A) Metaplots of H2Bub (green), Pob3 (orange), Spt16 (brown) and RNAPIISer2P (pink) ChIP-seq enrichment [log2(ChIP/Input)] aligned to the TSS +1 (left) or TTS -1 (right) nucleosome in wild-type strain. Scaled nucleosome density (wild-type) is plotted as grey shading. Highly expressed genes are considered (n = 1117 for TSS+1 and n = 917 for TTS-1). Average of 2 biological replicates is shown.

B) Example regions of Spt16 ChIP-seq profiles [log2(ChIP/Input)] at highly expressed genes (first and second) or at low-moderately expressed genes (third and fourth). Colors: grey – wild-type (WT); blue – *pob3Δ*. Two biological replicates are shown.

C) Metaplots of log2FC between *pob3Δ* vs. wild-type of Spt16 (brown) and RNAPIISer2P (pink) ChIP-seq, antisense transcripts from RNA-seq (red) and

nucleosome density (grey) aligned to the TSS +1 or TTS -1 nucleosome. Left: highly expressed genes (n = 1117 for TSS+1 and n = 917 for TTS-1); right: low-moderately expressed genes (n = 1132 for TSS+1 and n = 976 for TTS-1). Gene body nucleosome positions are marked with dashed vertical lines.

Figure 6. FACT regulates subtelomeric gene silencing, density of subtelomeric nucleosomes and knob formation.

A) Schematic representation of *S. pombe* chromosomes. Tel – subtelomeric heterochromatin, subTEL – knob regions, cen – centromere, rDNA – ribosomal DNA.

B) Scatterplots of RNA-seq log2FC (sense) between *pob3Δ* and wild-type for genes along chromosomal coordinates. Red line is calculated by 'loess' fitting.

C) Boxplots of RNA-seq log2FC (sense) between mutant vs. wild-type for genes in subtelomeric (n = 152) or nonsubtelomeric regions (n = 4917). Dotted horizontal line indicates no difference. Colors: orange – *H2BK119R* vs. wild-type (WT); blue – *pob3Δ* vs. wild-type (WT); magenta – *pob3Δ H2BK119R* vs. wild-type (WT).

D) Boxplots of Fold Change between mutant vs. wild-type nucleosome density averaged in a 150 bp window surrounding nucleosome center positions in subtelomeric (n = 2500) or nonsubtelomeric regions (n = 69154). Dotted horizontal line indicates no difference. Colors are same as in C.

E) Fraction of nuclei with 0, 1, 2 or 3 knobs (increasing grey colors) comparing wild-type to *H2BK119R*, *pob3Δ* and *pob3ΔH2BK119R* mutants. Knobs were calculated from three independent experiments (n=6 for WT) from several hundreds of nuclei. Error bars represent SEM.

F) Fraction of nuclei with 0, 1, 2 or 3 knobs comparing wild-type (*H3K36*) to *H3K36R*, *pob3ΔH3K36* and *pob3ΔH3K36R* mutants. Knobs were calculated from three independent experiments from several hundreds of nuclei. Error bars represent SEM.

Figure 7. A model of FACT and H2Bub cooperativity within gene bodies

In the *wt* strain, H2Bub facilitates histone deposition on DNA by FACT. In the *pob3Δ* strain, 5' antisense transcription (AS trxn) is de-repressed, the +1 nucleosome is destabilized, Spt16 maintains nucleosomes closer to 3' gene ends. In the *H2BK119R* mutant, FACT binds stronger histones and it is shifted downstream of TTS, the genic nucleosomes are less stable and genic AS trxn is de-repressed. Stabilization of the +1 nucleosome likely blocks AS trxn around 5' of the genes. In the double mutant, FACT bound histones are released and nucleosomes are correctly assembled suppressing genic AS trxn. A glow around nucleosomes depicts their dynamics; dashed lane around nucleosomes represents their reduced stability in a given mutant; orange oval - H2A-H2B dimer, yellow shape - ubiquitin.

STAR METHOD

LEAD CONTACT AND MATERIALS AVAILABILITY

Further information and requests for resources and reagents should be directed to and will be fulfilled by the Lead Contact, Andreas Ladurner (andreas.ladurner@bmc.med.lmu.de).

EXPERIMENTAL MODEL AND SUBJECT DETAILS

Strains used in this study are listed in **Table S1**. All strains were generated using standard procedures using yeast transformation and validated by PCR. All strains were grown in rich media (YES) at 30°C. For temperature sensitive alleles, strains were grown at 26°C overnight and then they were shifted to 36°C for 1.5-2 hours.

METHOD DETAILS

RNA extraction

RT-QPCR was done as described in (Barrales et al., 2016). Briefly, 50 ml of yeast culture at OD600 ~0.5-0.8 was spun down at RT and the pellet frozen in liquid nitrogen. Cells were thawed on ice and resuspended in 1 ml of TRIzol. 250 ul of zirconia beads were added and cells were broken with Precyllis 24 (Peqlab) for 3x30 s with 5 min rest on ice. The extract was spun down at 13500 rpm at 4°C for 10 min. The cleared lysate was extracted twice with chloroform and spun at 13500 rpm at 4°C for 10 min. The aqueous phase was taken and RNA was precipitated with isopropanol. The pellet was washed twice with 75% EtOH, air dried and resuspended in 50 μl of RNAse free dH20. The RNA concentration and purity was determined by Nano-drop.

cDNA synthesis

RT-QPCR was done as described in (Barrales et al., 2016). Briefly, 20 μg of RNA was treated with 1 μl of TURBO DNase I (Ambion) for 1 hr at 37°C. The reaction was inactivated by adding 6 μl of DNase inactivation reagent followed by the manufacturer instructions. For cDNA synthesis 5 μg of total DNase-treated RNA was reverse transcribed with 1μl of oligo-(dT)20 primers (50 μM) and 0.25 μl of SuperscriptIII (Invitrogen) according to the manufacturer instructions.

RT-QPCR

RT-QPCR was done as described in (Barrales et al., 2016). Briefly, immunoprecipitated DNA and cDNAs were quantified by qPCR using Fast SYBR Green Master mix (Life Technologies) and a 7500 Fast real-time PCR system (Applied Biosystems). cDNA was analyzed by qPCR using gene specific primers (**Table S2**). Amplifications were performed in at least 3 biological replicates. The quantification was based on a standard curve method obtained with QuantStudio™ Design and Analysis Software. Sheared *S. pombe* genomic DNA was used as a

standard. For gene expression the samples were normalized to *act1* gene. The normalized data sets were shown as relative to the mean value of the wild type strain which was set to 1, errors bars were calculated as SEM and displayed accordingly.

RNA-seq library preparation

RNA for RNA-seq was prepared as described above. 1 μg of RNA was treated with NEBNext®Poly(A) mRNA Magnetic Isolation Module to enrich for poly-adenylated transcripts. The libraries were prepared with NEBNext®Ultra™Directional RNA Library Prep Kit for Illumina® according to the manual instructions. The libraries were barcoded and sequenced at LAFUGA at the Gene Center.

RNA-seq analysis

RNA-seq 50 bp single reads were aligned to the reference genome (Schizosaccharomyces pombe ASM294v2) using STAR (version 2.5.3a). Uniquely mapped reads were counted per genes in sense or antisense orientation with STAR --quantMode GeneCounts using the annotation ASM294v2.37. Both sense and antisense read counts were normalized to the sense read counts using DESeq2 R package (version 1.18.1). Differential expression analysis was also performed by DESeq2 functions. Coverage vectors were generated from the BAM files (from STAR alignment) using Bioconductor packages and normalized to the total coverage. TSS aligned or gene body scaled matrices were calculated from the coverage vectors at protein coding genes. Further analysis was performed using R and graphs were plotted by R base graphics.

MNase-seq library preparation

500 ml of S. pombe cells were grown overnight at 30°C to OD600 ~ 0,5. Cells were crosslinked with 0.5% formaldehyde for 20 min at RT. The crosslinking was stopped with 125 mM Glycine. Cells were spun, washed with dH2O and the pellet was

resuspended in 20 ml of ice cold Preincubation solution (19.7 mM Na_2HPO_4, 109 mM citric acid, 40 mM EDTA, 28.6 mM b-Mercaptoethanol). The cells were incubated at 30°C with vigorous shaking for 10 min. Cells were harvested at 4000 rpm for 5 min at 4°C and the pellet was resuspended in 10 ml Sorbitol/Tris buffer (1M sorbitol, 50 mM Tris pH 7.4). 10 mg of Zymolyase 100T was added and the spheroplasts were incubated at 30°C for 30 min with vigorous shaking followed by centrifugation at 400 rpm for 5 min at 4°C. The spheroplasts were washed once with 40 ml Sorbitol/Tris buffer (ice cold, without b-Mercaptoethanol) and the pellet was resuspended in 7.5 ml of NP buffer (ice cold) with 1 mM b-Mercaptoethanol and 500 µM spermidine. Samples were split into 1 ml aliquots and various amounts of MNase (Sigma, 0.6 U/ml) were added (2,4,6,8,10 and 12 ul) and the samples were incubated at 37°C for 20 min. The reaction was stopped with 138 ul of Stop Buffer (5% SDS, 100 mM EDTA). Samples were digested with 40 ul of RNAse A (10mg/ml) at 37°C for 45 min. 50 ul of Proteinase K (20 mg/ml) was added and the samples were incubated O/N at 65°C. 360 ul of 3 M potassium acetate pH 5.5 was added to each sample, incubated on ice for 10 min and spun down at 14000 rpm, 4°C for10 min. Next, the samples were phenol/chloroform extracted and DNA was precipitated with 0.2M NaCl and Isopropanol, 1 ul of glycogen (20 mg/ml) was added as a carrier. After precipitation nucleosomal DNA was washed with 70% Ethanol, air dried and resuspended in 50 ul of TE. Samples were loaded on a 1.5% agarose gel (Biozym ME agarose) in 1 x TAE and resolved. Mononucleosmal DNA was cut out and DNA was recovered with Freeze N' Squeeze gel extraction columns (BioRad). DNA was precipitated with isopropanol in the presence of glycogen and the pellet was resuspended in 20 µl TE. DNA was kept at -20C until library preparation. The libraries were prepared with 50 ng of *S. pombe* mononucleoosmal DNA. All enzymes, buffers and primer sets were from NEB. Shortly, first DNA was end-repaired, followed by AMPure bead purification. DNA was then dA-tailed and purified with AMPure beads. Finally, the adaptor ligation was performed O/N at 16°C. The reaction was treated with USER

enzyme and purified with AMPure beads. Finally, the multiplexing PCR reaction was performed with a Phiusion polymerase. Usually 8 PCR cycles were performed to avoid the library over-amplification. PCR product was purified on a native 5% polyacrylamide gel and extracted in 400 μl of Gel Extraction Buffer (300 mM NaCl, 10 mM Tris pH 8.0, 1 mM EDTA) O/N at 4°C. Extracted DNA was further precipitated with isopropanol and the final library was resuspended in 15 ul of 0.1 TE. DNA was measured by Qubit DNA HS (Invitrogen) and the quality of the library was further verified by Bioanalyzer. The libraries were paired-end sequenced by LAFUGA (LMU).

MNase-seq analysis

MNase-seq 50 bp paired-end reads were aligned to the reference (Schizosaccharomyces pombe ASM294v2) using bowtie2 (version 2.2.9). Reads were filtered by samtools with -q 2 parameter (version 1.3.1). BAM alignments were converted to BEDPE format using bedtools2 (version 2.26.0), from which fragment coordinates were extracted and the number of fragments were subsampled to 6 million. Dyad coverages were calculated using the bed2dyad function from the tsTools R package (https://github.com/musikutiv/tsTools) with the width parameter 50 (version 0.1.0). Dyad coverages were normalized by the total coverage and multiplied by a million.Nucleosome reference positions were defined by DANPOS (version 2.2.2)(Chen et al., 2015) for each condition (i.e. genotype, MNase digestion degree) independently. Dyad coverages were aligned to wild type nucleosome positions that are within a 150 bp window downstream of TSS (TSS +1) or upstream of TTS (TTS -1). Orientation was determined by the strand of the underlying gene. For the H2AZ analysis, genes were subset by the overlap with H2AZ peaks, which were called by the Homer software package (Heinz et al., 2010) findPeaks command with paramters “-style histone -F 2” (H2AZ data source: GSE97984). Sub-telomeric

genes were defined by their localization to the following regions: chrI:30000-150000; chrI:5430000-5560000; chrII:30000-150000 and chrII:4390000-4500000. Further analysis was performed using R and graphs were plotted by R base graphics.

ChIP-seq

100 ml yeast cultures were grown to mid-log phase to OD_{600}=0.6. The cultures were cooled down at RT for 10 min and fixed with 1% FA for 20 min at RT on the shaker. Cross-linking was stopped with 150 mM Glycine for 10 min at RT on the shaker. Cells were spun down 2 min at 3000 rpm at 4°C, washed 2x with 30 ml cold dH2O, the pellet wash immediately frozen down in liquid nitrogen and kept at -80°C until further processing. Pellets were resuspended in 1 ml FA(1) buffer (50 mM Hepes-KOH, pH 7.5, 150 mM NaCl, 1 mM EDTA, 1% Triton X-100 (v/v) , 0,1% NaDeoxycholate (w/v) , 0,1% SDS (w/v)0 supplemented with Roche protease inhibitors and phosSTOP (Roche). Cells were broken in a bead beater (Precellys): 9x30s. After centrifugation, the supernatant and the pellet were sonicated for 15 min at 4°C. Chromatin extracts were spun down for 10 min at 14000 rpm at 4°C. Different amount of chromatin was used for different antibodies: 100 ul chromatin (for H3, Spt16, Pob3 ChIP) or 500 ul chromatin (for RNAPIISer2, H3K9me2, H2Bub ChIP). The antibodies used for ChIP are listed in Key Resources Table. Samples were incubated with antibodies O/N at 4°C on the wheel. 25 ul of FA(1) buffer washed Dynabeads were added to each sample and they were incubated for 2 hours at 4°C on the wheel. Samples were then washed 3x for 5 min at RT with FA(1) buffer, FA(2) buffer (FA(1) buffer with 500 mM NaCl), once with LiCl buffer (10 mM TrisHCl, pH 8.0, 0.25 M LiCl, 1 mM EDTA, 0,5% NP-40 (v/v) , 0,5% NaDeoxycholate (w/v)) and once with TE buffer. DNA was eluted from the antibodies with ChIP Elution buffer (50 mM Tris HCl, pH 7.5, 10 mM EDTA, 1% SDS) for 15 min at 65°C in a thermomixer set to 1300 rpm. DNA was treated with RNAseA (Thermo Fisher) for 1 hr at 37°C,

followed by Proteinase K digestion and de-crosslinking O/N at 65°C. DNA was purified with Zymo Research ChIP DNA Clean and Concentrator kit according to the manual instructions. To obtain enough material for the library preparation usually 3 technical IP replicates were pulled. The ChIP-seq libraries were prepared with 2 ng of DNA with NEBNext®Ultra™ II DNA Library Prep Kit for Illumina® according to the manual instructions. The libraries were barcoded and sequenced at LAFUGA at the Gene Center (LMU).

ChIP-seq analysis

ChIP-seq 50 bp single-end reads were aligned to the reference (Schizosaccharomyces pombe ASM294v2) using bowtie2 (version 2.2.9). Reads were processed using the Homer software package (Heinz et al., 2010). Tag directories were created with the parameter -mapq 1 and bedgraph coverages were generated and normalized to the total number of reads and to the corresponding input using the makeUCSCfile command. Normalized coverages were aligned to gene bodies (similar to RNA-seq) or to TSS +1, TTS -1 nucleosome positions (similar to MNase-seq). Further analysis was performed using R and graphs were plotted by R base graphics.

Whole cell extracts (WCE)

50 ml yeast cultures were grown to mid-log phase (OD_{600} 0.5-0.8). The cultures were spun down and washed once with cold dH_20. Cell pellets were resuspended in 500 µl of Workman Extract Buffer (40mM HEPEs pH7.4, 250mM NaCl, 0.1% NP40, 10% Glycerol, 1 mM PMSF, Roche proteinase inhibitors). 250 µl of glass beads were added and cells were lysed with Peqlab precellys homogenizator (3x30 sec with 2 min on ice incubation in between). The extracts were shortly spun down at 2500 rpm at 4°C for 3 min. The supernatant and the pellet were treated with benzonase in the

presence of 2mM $MgCl_2$ for 30 min on ice and spun down at the maximum speed for 10 min at 4°C. The extracts were frozen down in liquid nitrogen and kept at -80°C or immediately used for immunoprecipitation. Protein concentration was measured with Bradford reagent (BioRad).

Immunoprecipitation

500 μg of WCE was incubated with 7.5 μl Flag beads (Sigma) for 2 hours at 4°C. The beads were washed three times for 5 min with Workman Extract Buffer with the indicated salt concentrations. Precipitated proteins were eluted for 30 min on ice with 20 μl of 250 μg/ml 3xFlag peptide (Sigma) in Elution Buffer (40mM HEPEs pH7.4, 100mM NaCl, 0.1% NP40, 10% Glycerol, 1 mM PMSF, Roche proteinase inhibitors).

Western Blot

Proteins were separated with SDS–polyacrylamide gel electrophoresis (SDS–PAGE) and electroblotted onto methanol activated polyvinylidene difluoride (PVDF) membranes in Blotting Buffer (20 mM Tris, 192 mM glycin, 20% methanol) for 1hr at 400 mA at 4°C. Membranes were then incubated in Blocking Buffer (TBS, 0.1% Tween 20, 5% non-fat dry milk) for 40 min - 1hr at room temperature followed by an incubation in the Blocking Buffer with an appropriate primary antibody for 1hr at RT. Membranes were washed three times for 5 min in Washing Buffer - TBST (TBS, 0.1% Tween 20) and then incubated in Blocking Buffer containing the appropriate secondary antibody for 40 min at room temperature followed by 3 times washing in TBST for 5 min. Western blot signals were visualized by chemiluminescence using the Immobilon Western Chemiluminescence HRP substrate (Millipore, WBKLS0500) on X-ray films (Fujix Super RX 13x18). For quantification of Western blots fluorescently labeled secondary antibodies were used and the membranes were

scanned with LiCor Imaging System. The scans were analyzed with Image Studio Lite software.

Super-resolution microscopy

S. pombe cells were cultured in liquid minimum medium with supplements (EMM2 5S) at 26 ˚C with shaking to the early logarithmic phase. Alternatively, for heat shock experiments, cells were cultured in liquid YES medium at 26 ˚C over night and shifted to 36 ˚C for 1.5-2 hours. Cells were pelleted by gentle centrifugation, and chemically fixed by re-suspending in a buffer containing 4 % formaldehyde (Polysciences, Inc., USA), 80 mM HEPES-K, 35 mM HEPES-Na, 2 mM EDTA, 0.5 mM EGTA, 0.5 mM spermidine, 0.2 mM spermine and 15 mM 2-mercaptethanol, pH 7.0. After fixation for 10 min at room temperature, cells were washed with PEMS (100 mM PIPES, 1 mM EGTA, 1 mM $MgSO_4$, 1.2 M sorbitol pH 6.9) three times, then, digested with 0.6 mg ml^{-1} zymolyase 100T (Nacalai Tesque, Japan) in PEMS at 36 ˚C for 5 min for DAPI staining and 60 min for immunostaining. Next, cells were treated with 0.1% triton X-100 in PEMS for 5 min, and washed three times thereafter with PEMS. For DAPI staining, cells were incubated with 0.2 µg ml^{-1} DAPI in PEMS for 10 min, and then cells were resuspended with nPG-Glycerol (100 % glycerol for absorptionmetric-analysis (Wako, Japan) with 4 % n-propyl gallate, pH 7.0) and mounted on a clean 18x18 mm coverslip of thickness 0.16-0.19 mm (Matsunami, Japan). For immunostaining, cells were incubated with 1% BSA, 0.1 % NaN3, 100 mM L-lysine monohydrochloride in PEMS (PEMSBAL) for 30 min, and the solution was replaced with H2BK120ub antibody (Active Motif) diluted to 1/1,000 in PEMSBAL and incubated for 1 h. Cells were washed with PEMSBAL three times then anti-mouse IgG antibody with Alexa Fluor 488 (Thermo Fisher Scientific, USA) diluted to 1/500 in PEMSBAL was added. Afterwards, the cells were washed, counter-stained with DAPI and suspended in mounting medium (nPG-Glycerol, see above). The slides were analyzed with 3D-SIM using a DeltaVision|OMX SR

microscope (GE Healthcare, UK) equipped with a 60x PlanApoN NA1.42 oil immersion objective lens (Olympus, Japan). Reconstruction of 3D-SIM was performed by softWoRx (GE Healthcare) with Wiener filter constants of 0.002 using a homemade optical transfer function. Conspicuously condensed, DAPI-stained bodies were counted as knobs by visually inspecting each optical section of 3D-SIM images. Chromatic shift of multicolor images was measured by Chromagnon v0.80 (Matsuda et al., 2018) using image stacks of cells stained with DAPI and H2Bub, and the global alignment parameters thus obtained were applied to the original image stacks.

Chaperoning assay

A typical reaction was performed in 10 ul volume. Recombinant human FACT (150 nM) was pre-incubated with wild type or ubiquitinated histone octamers (46.3 nM) in an assembly buffer (20 mM Tris-HCl pH 8.0, 0.1 mM EDTA, 1 mM DTT, 10% glycerol) for 30 min at 37°C. 601 DNA with 30 bp overhangs (11.2 nM) was added in suboptimal concentration (1:4 molar DNA:histone ratio) and the reaction was incubated further for 30 min at 37°C. The samples were spun down at a maximum speed for 15 seconds and the supernatant was loaded on 6% native PAA gel. The electrophoresis was performed in 0.4xTAE buffer. The gel was pre-run for minimum 30 min and the samples were resolved for 70 min at 100 V at RT using XCell SureLock®MiniCell system (Invitrogen). The gel was scanned with Typhoon FLA 9500 with Cy3 filter. The signals were analyzed with Image Studio Lite software. Each assay was performed independently three times, each sample was run in three technical replicates within the assay.

Recombinant FACT purification

Recombinant human FACT was purified similarly as published before (Tsunaka et al., 2016) with some modifications (Figure S5F). Briefly, His-tagged SSRP1 and Flag-tagged Spt16 were coexpressed in SF21 cells. A pellet from 2.5 - 5 liters of SF21 cells was resuspended in Lysis Buffer (300 mM NaCl, 20 mM Hepes pH 7.4, 30 mM imidazole, 10% glycerol, supplemented with Roche inhibitors, PMSF and 0.5 mM TCEP). Cells were lysed by 3 cycles of freeze and thaw in liquid nitrogen. The extract was briefly sonicated (4x10 seconds) and spun down 40 min at 25.000 rpm in the Beckman centrifuge. The extract was loaded on the HisTrap HP Column and washed with High Salt Wash Buffer (1M NaCl, 20 mM Hepes pH 7.4, 30 mM imidazole, 10% glycerol, 0.5 mM TCEP) and eluted with Elution Buffer (300 mM NaCl, 20 mM Hepes pH 7.4, 500 mM imidazole, 10% glycerol, 0.5 mM TCEP). Fractions containing hFACT were pooled and treated with 100 U of Antarctic Phosphatase for 1hr on ice. The salt was diluted in the extract to 150 mM NaCl and the extract was loaded on the Resource Q column. The column was eluted with a 0-75% gradient by mixing 150 mM with 1M NaCl buffer. The fractions containing hFACT were frozen in liquid nitrogen and the next day they were concentrated on the Amicon 10K and loaded on the preparative size exclusion column (HiLoad 26/60 Superdex 200) in the Size Exclusion buffer (250 mM NaCl, 20 mM Hepes pH 7.4, 10% glycerol, 0.5 mM TCEP). Fractions containing hFACT were pooled, concentrated, aliquoted and stored at -80°C.

Histone purification and modification

Human histones H2A, H2B and H2B K120C were purified essentially as described (Dyer et al, 2004 methods enzymology, Wilson and Benlekbir Nature 2016). Briefly, histones were expressed in BL-21(DE3) RIL cells and expressed histones purified from insoluble inclusion bodies on a HiTrap SP XL column (GE Healthcare). Histone fractions were pooled and dialyzed extensively against 1 mM acetic acid solution prior to lyophilization. Mutant human Histone H2B engineered with a single cross-

linkable cysteine (H2B K120C) was chemically ubiquitylated essentially as described (Long et al., 2014; Wilson et al., 2016). Briefly, an alkylation reaction was assembled with H2B K120C (700 uM), His-TEV-ubiquitin G76C (700 uM) and 1,3-dibromoacetone (4.2 mM, Santa Cruz) in 250 mM Tris-Cl pH 8.6, 8 M urea and 5 mM TCEP and the reaction was allowed to proceed for 16 hours on ice. The reaction was quenched by the addition of 10 mM β-mercaptoethanol and pH adjusted to 7.5. chemically ubiquitylated H2B (H2B Kc120ub) was purified using a HiTrap SP HP column (GE Healthcare) and HisTEV-H2AKc120ub containing fractions were pooled and enriched over a HiTrap chelating column (GE Healthcare) pre-loaded with Ni^{2+} ions. The 6xHis tag was removed by TEV cleavage and subsequent Ni^{2+} column subtraction. The resulting flow-through was dialysed against a 2 mM β-mercaptoethanol/dH20 solution and lyophilized. Lyophilized H2A and H2B or H2B K120ub were resuspended at roughly 5mg/ml in 7 M Guanidine hydrochloride, 20 mM Tris pH 7.5, 5mM DTT. Histones were mixed at equimolar ratios, diluted to roughly 2 mg/ml and extensively dialyzed in 2M NaCl, 20 mM Tris pH 7.5, 5 mM β-mercaptoethanol, 2 mM EDTA. Dimers were purified by Size exclusion chromatography using a Superdex 200 Increase 10/300 column and fractions corresponding to H2A/H2B dimers pooled and concentrated using Amicon Ultra 10kDa MWCO spin concentrators (Millipore). Dimers were diluted 1:1 (v/v) with 100% glycerol for storage at -20°C (Figure S5C).

EMSA

0.8 μM FACT complex was incubated with increased amounts of unmodified or ubiquitinated histone H2A-H2B dimers in the binding buffer (20 mM Hepes pH 7.4, 145 mM NaCl, 10% glycerol, 1 mM DTT) for 1 hour at 37°C. Samples were loaded on pre-run 5.5% 0.4xTBE native PAA gel and the gel was run at 100V for 70 min at RT in 0.4xTBE running buffer. Gels were stained with InstantBlue™ (Expedeon) for

30 min, rinsed in dH20 and scanned with Labscan. The unbound FACT bands were quantified with Image Studio™ Lite software and a dose-response curve was generated using GraphPad Prism V8.1.2 (Nonlinear fit, Agonist vs. response, variable slope (four parameters) from 3 independent experiments. Error shows SDEV.

QUANTIFICATION AND STATISTICAL ANALYSIS

Quantification and statistical tests employed for each experiment are described in the figure legends or in the method section. For RNA-seq, MNase-seq and ChIP-seq experiments, two biological replicates were sequenced for each condition.

DATA AND CODE AVAILABILITY

All raw sequencing datasets were deposited to NCBI GEO with the accession number: GSE124092. R code for data analysis is available upon request. Raw image data are available at Mendeley: http://dx.doi.org/10.17632/jvb77prdgv.1

References

Barrales, R.R., Forn, M., Georgescu, P.R., Sarkadi, Z., and Braun, S. (2016). Control of heterochromatin localization and silencing by the nuclear membrane protein Lem2. Genes Dev *30*, 133-148.

Batta, K., Zhang, Z., Yen, K., Goffman, D.B., and Pugh, B.F. (2011). Genome-wide function of H2B ubiquitylation in promoter and genic regions. Genes Dev *25*, 2254-2265.

Belotserkovskaya, R., Oh, S., Bondarenko, V.A., Orphanides, G., Studitsky, V.M., and Reinberg, D. (2003). FACT facilitates transcription-dependent nucleosome alteration. Science *301*, 1090-1093.

Buchanan, L., Durand-Dubief, M., Roguev, A., Sakalar, C., Wilhelm, B., Stralfors, A., Shevchenko, A., Aasland, R., Shevchenko, A., Ekwall, K.*, et al.* (2009). The Schizosaccharomyces pombe JmjC-protein, Msc1, prevents H2A.Z localization in centromeric and subtelomeric chromatin domains. PLoS Genet *5*, e1000726.

Chandrasekharan, M.B., Huang, F., and Sun, Z.W. (2009). Ubiquitination of histone H2B regulates chromatin dynamics by enhancing nucleosome stability. Proc Natl Acad Sci U S A *106*, 16686-16691.

Chen, K., Chen, Z., Wu, D., Zhang, L., Lin, X., Su, J., Rodriguez, B., Xi, Y., Xia, Z., Chen, X.*, et al.* (2015). Broad H3K4me3 is associated with increased transcription elongation and enhancer activity at tumor-suppressor genes. Nat Genet *47*, 1149-1157.

Clark-Adams, C.D., and Winston, F. (1987). The SPT6 gene is essential for growth and is required for delta-mediated transcription in Saccharomyces cerevisiae. Mol Cell Biol *7*, 679-686.

Dann, G.P., Liszczak, G.P., Bagert, J.D., Muller, M.M., Nguyen, U.T.T., Wojcik, F., Brown, Z.Z., Bos, J., Panchenko, T., Pihl, R.*, et al.* (2017). ISWI chromatin remodellers sense nucleosome modifications to determine substrate preference. Nature *548*, 607-611.

Debelouchina, G.T., Gerecht, K., and Muir, T.W. (2016). Ubiquitin utilizes an acidic surface patch to alter chromatin structure. Nature Chemical Biology *13*, 105-110.

Dinant, C., Ampatziadis-Michailidis, G., Lans, H., Tresini, M., Lagarou, A., Grosbart, M., Theil, A.F., van Cappellen, W.A., Kimura, H., Bartek, J.*, et al.* (2013). Enhanced chromatin dynamics by FACT promotes transcriptional restart after UV-induced DNA damage. Mol Cell *51*, 469-479.

Duina, A.A., Rufiange, A., Bracey, J., Hall, J., Nourani, A., and Winston, F. (2007). Evidence that the localization of the elongation factor Spt16 across transcribed genes is dependent upon histone H3 integrity in Saccharomyces cerevisiae. Genetics *177*, 101-112.

Dobin, A., Davis, C.A., Schlesinger, F., Drenkow, J., Zaleski, C., Jha, S., Batut, P., Chaisson, M., and Gingeras, T.R. (2013). STAR: ultrafast universal RNA-seq aligner. Bioinformatics *29*, 15-21.

Feng, J., Gan, H., Eaton, M.L., Zhou, H., Li, S., Belsky, J.A., MacAlpine, D.M., Zhang, Z., and Li, Q. (2016). Noncoding Transcription Is a Driving Force for Nucleosome Instability in spt16 Mutant Cells. Mol Cell Biol *36*, 1856-1867.

Fleming, A.B., Kao, C.-F., Hillyer, C., Pikaart, M., and Osley, M.A. (2008). H2B Ubiquitylation Plays a Role in Nucleosome Dynamics during Transcription Elongation. Molecular Cell *31*, 57-66.

Flury, V., Georgescu, P.R., Iesmantavicius, V., Shimada, Y., Kuzdere, T., Braun, S., and Buhler, M. (2017). The Histone Acetyltransferase Mst2 Protects Active Chromatin from Epigenetic Silencing by Acetylating the Ubiquitin Ligase Brl1. Mol Cell *67*, 294-307 e299.

Garcia, H., Fleyshman, D., Kolesnikova, K., Safina, A., Commane, M., Paszkiewicz, G., Omelian, A., Morrison, C., and Gurova, K. (2011). Expression of FACT in mammalian tissues suggests its role in maintaining of undifferentiated state of cells. Oncotarget *2*, 783-796.

Guillemette, B., Bataille, A.R., Gevry, N., Adam, M., Blanchette, M., Robert, F., and Gaudreau, L. (2005). Variant histone H2A.Z is globally localized to the promoters of inactive yeast genes and regulates nucleosome positioning. PLoS Biol *3*, e384.

Gurova, K., Chang, H.W., Valieva, M.E., Sandlesh, P., and Studitsky, V.M. (2018). Structure and function of the histone chaperone FACT - Resolving FACTual issues. Biochim Biophys Acta. doi: 10.1016/j.bbagrm.2018.07.008

Hammond, C.M., Stromme, C.B., Huang, H., Patel, D.J., and Groth, A. (2017). Histone chaperone networks shaping chromatin function. Nat Rev Mol Cell Biol *18*, 141-158.

Hartzog, G.A., and Quan, T.K. (2008). Just the FACTs: histone H2B ubiquitylation and nucleosome dynamics. Mol Cell *31*, 2-4.

Heinz, S., Benner, C., Spann, N., Bertolino, E., Lin, Y.C., Laslo, P., Cheng, J.X., Murre, C., Singh, H., and Glass, C.K. (2010). Simple combinations of lineage-determining transcription factors prime cis-regulatory elements required for macrophage and B cell identities. Mol Cell *38*, 576-589.

Heo, K., Kim, H., Choi, S.H., Choi, J., Kim, K., Gu, J., Lieber, M.R., Yang, A.S., and An, W. (2008). FACT-Mediated Exchange of Histone Variant H2AX Regulated by Phosphorylation of H2AX and ADP-Ribosylation of Spt16. Molecular Cell *30*, 86-97.

Herrera-Moyano, E., Mergui, X., Garcia-Rubio, M.L., Barroso, S., and Aguilera, A. (2014). The yeast and human FACT chromatin-reorganizing complexes solve R-loop-mediated transcription-replication conflicts. Genes Dev *28*, 735-748.

Hodges, A.J., Gloss, L.M., and Wyrick, J.J. (2017). Residues in the Nucleosome Acidic Patch Regulate Histone Occupancy and Are Important for FACT Binding in Saccharomyces cerevisiae. Genetics *206*, 1339-1348.

Hondele, M., Stuwe, T., Hassler, M., Halbach, F., Bowman, A., Zhang, E.T., Nijmeijer, B., Kotthoff, C., Rybin, V., Amlacher, S.*, et al.* (2013). Structural basis of histone H2A-H2B recognition by the essential chaperone FACT. Nature *499*, 111-114.

Jeronimo, C., Watanabe, S., Kaplan, Craig D., Peterson, Craig L., and Robert, F. (2015). The Histone Chaperones FACT and Spt6 Restrict H2A.Z from Intragenic Locations. Molecular Cell *58*, 1113-1123.

Karolin Luger, A.W.M., Robin K. Richmond, David F. Sargent, Timothy J. Richmond (1997). Crystal structure of the nucleosome core particle at 2.8 Å resolution. Nature *389*.

Kemble, D.J., McCullough, L.L., Whitby, F.G., Formosa, T., and Hill, C.P. (2015). FACT Disrupts Nucleosome Structure by Binding H2A-H2B with Conserved Peptide Motifs. Mol Cell *60*, 294-306.

Kolundzic, E., Ofenbauer, A., Bulut, S.I., Uyar, B., Baytek, G., Sommermeier, A., Seelk, S., He, M., Hirsekorn, A., Vucicevic, D.*, et al.* (2018). FACT Sets a Barrier for Cell Fate Reprogramming in Caenorhabditis elegans and Human Cells. Dev Cell *46*, 611-626.e12.

Langmead, B., and Salzberg, S.L. (2012). Fast gapped-read alignment with Bowtie 2. Nat Methods *9*, 357-359.

Larochelle, M., Robert, M.A., Hebert, J.N., Liu, X., Matteau, D., Rodrigue, S., Tian, B., Jacques, P.E., and Bachand, F. (2018). Common mechanism of transcription termination at coding and noncoding RNA genes in fission yeast. Nat Commun *9*, 4364.

Lee, J., Choi, E.S., Seo, H.D., Kang, K., Gilmore, J.M., Florens, L., Washburn, M.P., Choe, J., Workman, J.L., and Lee, D. (2017). Chromatin remodeller Fun30(Fft3) induces nucleosome disassembly to facilitate RNA polymerase II elongation. Nat Commun *8*, 14527.

Lee, J.S., Garrett, A.S., Yen, K., Takahashi, Y.H., Hu, D., Jackson, J., Seidel, C., Pugh, B.F., and Shilatifard, A. (2012). Codependency of H2B monoubiquitination and nucleosome reassembly on Chd1. Genes Dev *26*, 914-919.

Lejeune, E., Bortfeld, M., White, S.A., Pidoux, A.L., Ekwall, K., Allshire, R.C., and Ladurner, A.G. (2007). The chromatin-remodeling factor FACT contributes to centromeric heterochromatin independently of RNAi. Curr Biol *17*, 1219-1224.

Li, H., Handsaker, B., Wysoker, A., Fennell, T., Ruan, J., Homer, N., Marth, G., Abecasis, G., Durbin, R., and Genome Project Data Processing, S. (2009). The Sequence Alignment/Map format and SAMtools. Bioinformatics *25*, 2078-2079.

Li, Y., Zeng, S.X., Landais, I., and Lu, H. (2007). Human SSRP1 has Spt16-dependent and -independent roles in gene transcription. J Biol Chem *282*, 6936-6945.

Long, L., Furgason, M., and Yao, T. (2014). Generation of nonhydrolyzable ubiquitin-histone mimics. Methods *70*, 134-138.

Love, M.I., Huber, W., and Anders, S. (2014). Moderated estimation of fold change and dispersion for RNA-seq data with DESeq2. Genome Biol *15*, 550.

Mata, J., Lyne, R., Burns, G., and Bahler, J. (2002). The transcriptional program of meiosis and sporulation in fission yeast. Nat Genet *32*, 143-147.

Matsuda, A., Chikashige, Y., Ding, D.Q., Ohtsuki, C., Mori, C., Asakawa, H., Kimura, H., Haraguchi, T., and Hiraoka, Y. (2015). Highly condensed chromatins are formed adjacent to subtelomeric and decondensed silent chromatin in fission yeast. Nat Commun *6*, 7753.

Matsuda, A., Schermelleh, L., Hirano, Y., Haraguchi, T., and Hiraoka, Y. (2018). Accurate and fiducial-marker-free correction for three-dimensional chromatic shift in biological fluorescence microscopy. Sci Rep *8*, 7583.

Mattiroli, F., D'Arcy, S., and Luger, K. (2015). The right place at the right time: chaperoning core histone variants. EMBO Rep *16*, 1454-1466.

Mayer, A., Lidschreiber, M., Siebert, M., Leike, K., Soding, J., and Cramer, P. (2010). Uniform transitions of the general RNA polymerase II transcription complex. Nat Struct Mol Biol *17*, 1272-1278.

McCullough, L.L., Pham, T.H., Parnell, T.J., Connell, Z., Chandrasekharan, M.B., Stillman, D.J., and Formosa, T. (2019). Establishment and Maintenance of Chromatin Architecture Are Promoted Independently of Transcription by the Histone Chaperone FACT and H3-K56 Acetylation in Saccharomyces cerevisiae. Genetics *211*, 877-892.

McGinty, R.K., Kohn, M., Chatterjee, C., Chiang, K.P., Pratt, M.R., and Muir, T.W. (2009). Structure-activity analysis of semisynthetic nucleosomes: mechanistic insights into the stimulation of Dot1L by ubiquitylated histone H2B. ACS Chem Biol *4*, 958-968.

Mieczkowski, J., Cook, A., Bowman, S.K., Mueller, B., Alver, B.H., Kundu, S., Deaton, A.M., Urban, J.A., Larschan, E., Park, P.J.*, et al.* (2016). MNase titration reveals differences between nucleosome occupancy and chromatin accessibility. Nat Commun *7*, 11485.

Nissen, K.E., Homer, C.M., Ryan, C.J., Shales, M., Krogan, N.J., Patrick, K.L., and Guthrie, C. (2017). The histone variant H2A.Z promotes splicing of weak introns. Genes Dev *31*, 688-701.

Nune, M., Morgan, M.T., Connell, Z., McCullough, L., Jbara, M., Sun, H., Brik, A., Formosa, T., and Wolberger, C. (2019). FACT and Ubp10 collaborate to modulate H2B deubiquitination and nucleosome dynamics. Elife *8*: e40988.

Orphanides, G., LeRoy, G., Chang, C.H., Luse, D.S., and Reinberg, D. (1998). FACT, a factor that facilitates transcript elongation through nucleosomes. Cell *92*, 105-116.

Pavri, R., Zhu, B., Li, G., Trojer, P., Mandal, S., Shilatifard, A., and Reinberg, D. (2006). Histone H2B Monoubiquitination Functions Cooperatively with FACT to Regulate Elongation by RNA Polymerase II. Cell *125*, 703-717.

Quinlan, A.R., and Hall, I.M. (2010). BEDTools: a flexible suite of utilities for comparing genomic features. Bioinformatics *26*, 841-842.

Sanso, M., Lee, K.M., Viladevall, L., Jacques, P.E., Page, V., Nagy, S., Racine, A., St Amour, C.V., Zhang, C., Shokat, K.M.*, et al.* (2012). A positive feedback loop links opposing functions of P-TEFb/Cdk9 and histone H2B ubiquitylation to regulate transcript elongation in fission yeast. PLoS Genet *8*, e1002822.

Segala, G., Bennesch, M.A., Pandey, D.P., Hulo, N., and Picard, D. (2016). Monoubiquitination of Histone H2B Blocks Eviction of Histone Variant H2A.Z from Inducible Enhancers. Mol Cell *64*, 334-346.

Sundaramoorthy, R., Hughes, A.L., El-Mkami, H., Norman, D.G., Ferreira, H., and Owen-Hughes, T. (2018). Structure of the chromatin remodelling enzyme Chd1 bound to a ubiquitinylated nucleosome. Elife *7*: e35720.

Suzuki, S., Kato, H., Suzuki, Y., Chikashige, Y., Hiraoka, Y., Kimura, H., Nagao, K., Obuse, C., Takahata, S., and Murakami, Y. (2016). Histone H3K36 trimethylation is essential for multiple silencing mechanisms in fission yeast. Nucleic Acids Res *44*, 4147-4162.

Tashiro, S., Handa, T., Matsuda, A., Ban, T., Takigawa, T., Miyasato, K., Ishii, K., Kugou, K., Ohta, K., Hiraoka, Y.*, et al.* (2016). Shugoshin forms a specialized

chromatin domain at subtelomeres that regulates transcription and replication timing. Nature Communications *7*, 10393.

Tanny, J.C., Erdjument-Bromage, H., Tempst, P., and Allis, C.D. (2007). Ubiquitylation of histone H2B controls RNA polymerase II transcription elongation independently of histone H3 methylation. Genes Dev *21*, 835-847.

True, J.D., Muldoon, J.J., Carver, M.N., Poorey, K., Shetty, S.J., Bekiranov, S., and Auble, D.T. (2016). The Modifier of Transcription 1 (Mot1) ATPase and Spt16 Histone Chaperone Co-regulate Transcription through Preinitiation Complex Assembly and Nucleosome Organization. J Biol Chem *291*, 15307-15319.

Trujillo, K.M., and Osley, M.A. (2012). A role for H2B ubiquitylation in DNA replication. Mol Cell *48*, 734-746.

Tsunaka, Y., Fujiwara, Y., Oyama, T., Hirose, S., and Morikawa, K. (2016). Integrated molecular mechanism directing nucleosome reorganization by human FACT. Genes Dev *30*, 673-686.

Van Oss, S.B., Shirra, M.K., Bataille, A.R., Wier, A.D., Yen, K., Vinayachandran, V., Byeon, I.-J.L., Cucinotta, C.E., Héroux, A., Jeon, J.*, et al.* (2016). The Histone Modification Domain of Paf1 Complex Subunit Rtf1 Directly Stimulates H2B Ubiquitylation through an Interaction with Rad6. Mol. Cell *64*, 815-825.

Warren, C., and Shechter, D. (2017). Fly Fishing for Histones: Catch and Release by Histone Chaperone Intrinsically Disordered Regions and Acidic Stretches. J Mol Biol *429*, 2401-2426.

Wilson, M.D., Benlekbir, S., Fradet-Turcotte, A., Sherker, A., Julien, J.P., McEwan, A., Noordermeer, S.M., Sicheri, F., Rubinstein, J.L., and Durocher, D. (2016). The structural basis of modified nucleosome recognition by 53BP1. Nature *536*, 100-103.

Winkler, D.D., Muthurajan, U.M., Hieb, A.R., and Luger, K. (2011). Histone chaperone FACT coordinates nucleosome interaction through multiple synergistic binding events. J Biol Chem *286*, 41883-41892.

Wittmeyer, J., and Formosa, T. (1997). The Saccharomyces cerevisiae DNA polymerase alpha catalytic subunit interacts with Cdc68/Spt16 and with Pob3, a protein similar to an HMG1-like protein. Mol Cell Biol *17*, 4178-4190.

Figure1

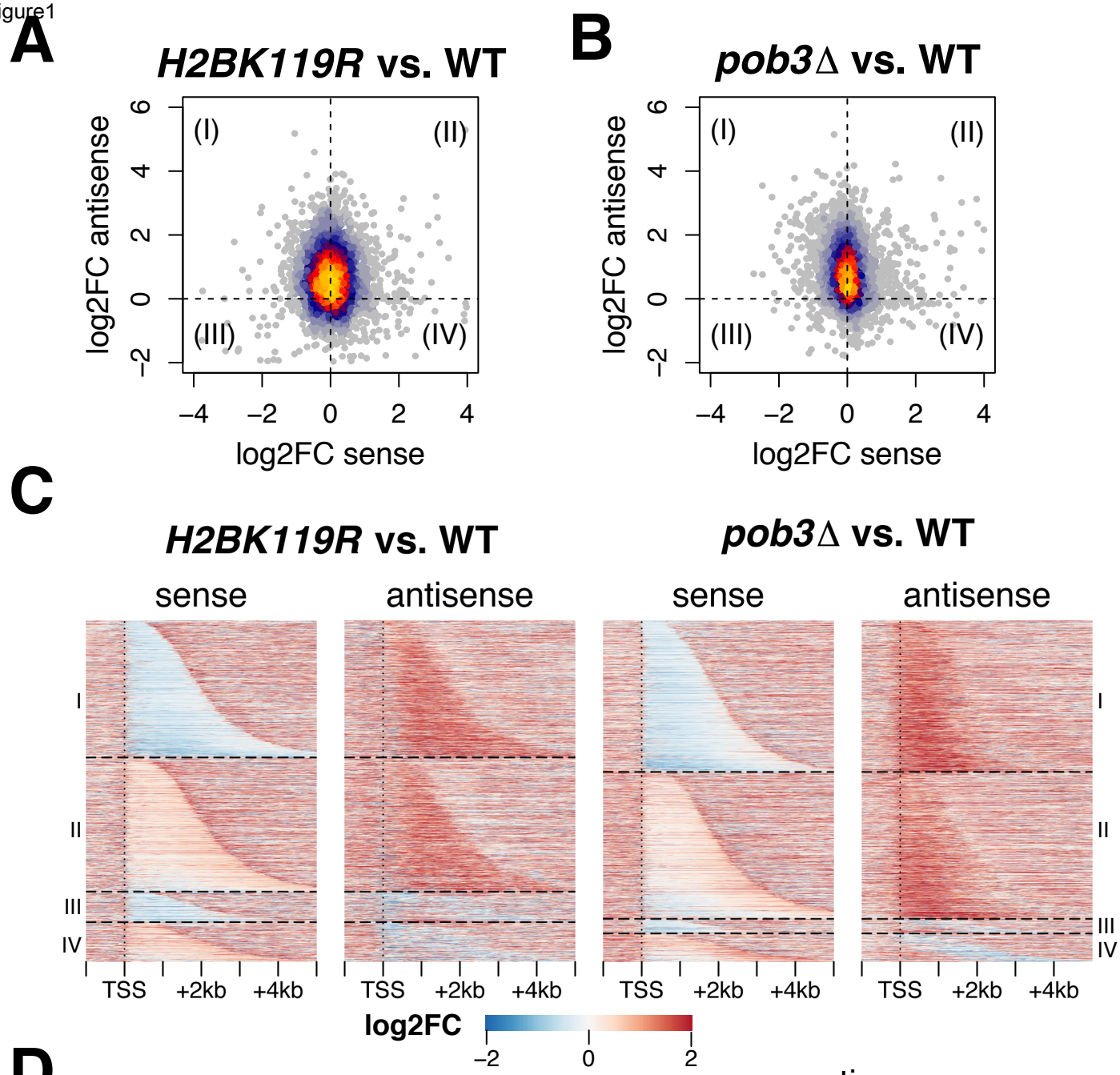

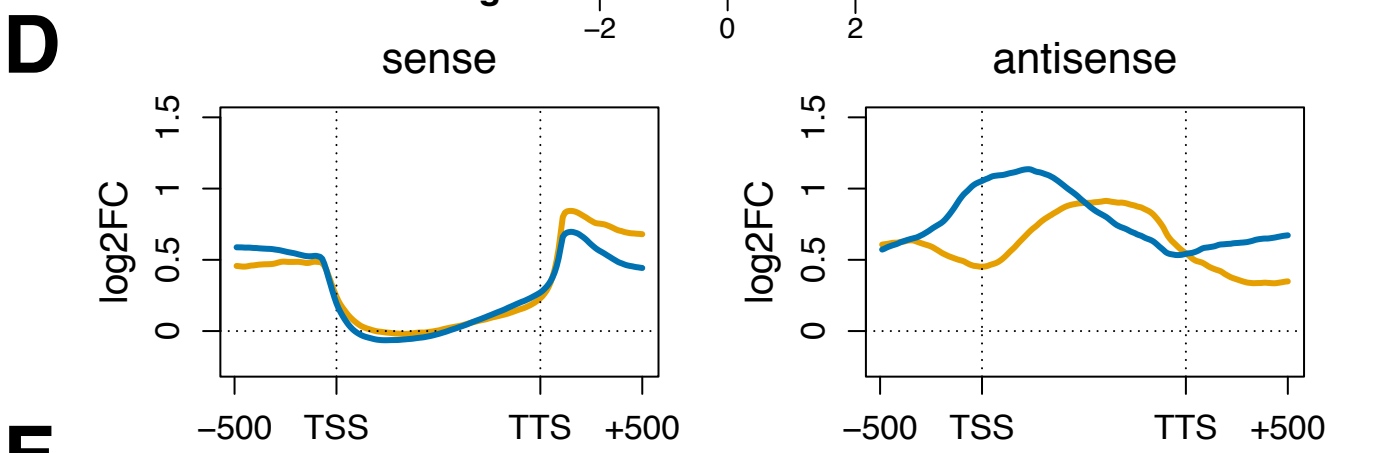

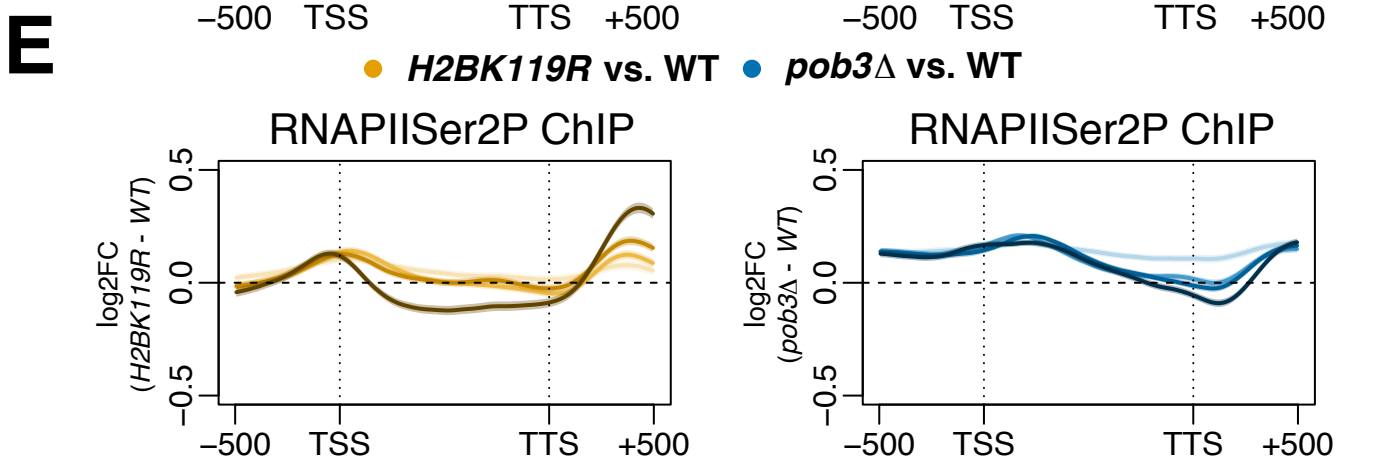

Figure 1

Figure2

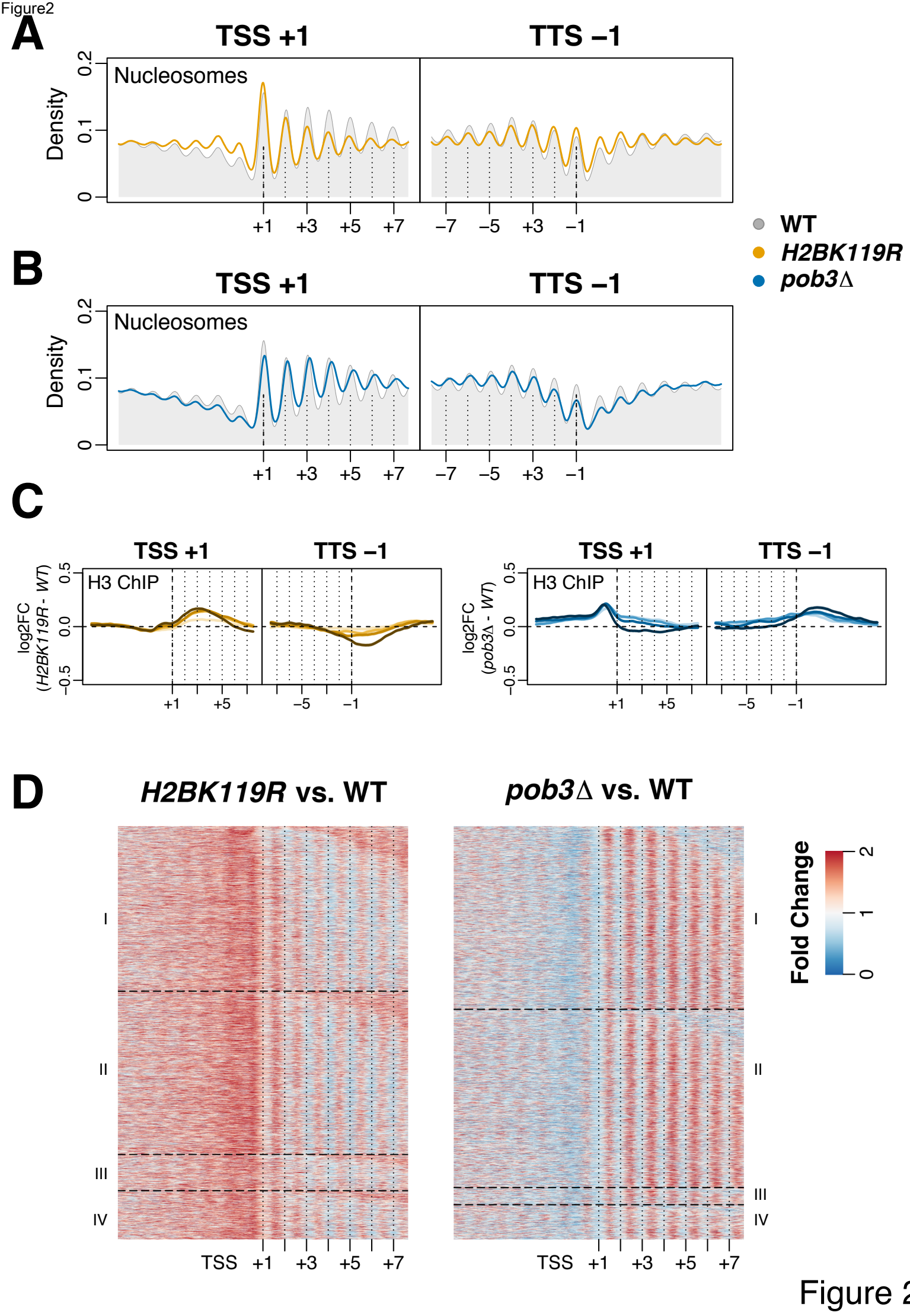

Figure 2

Figure3

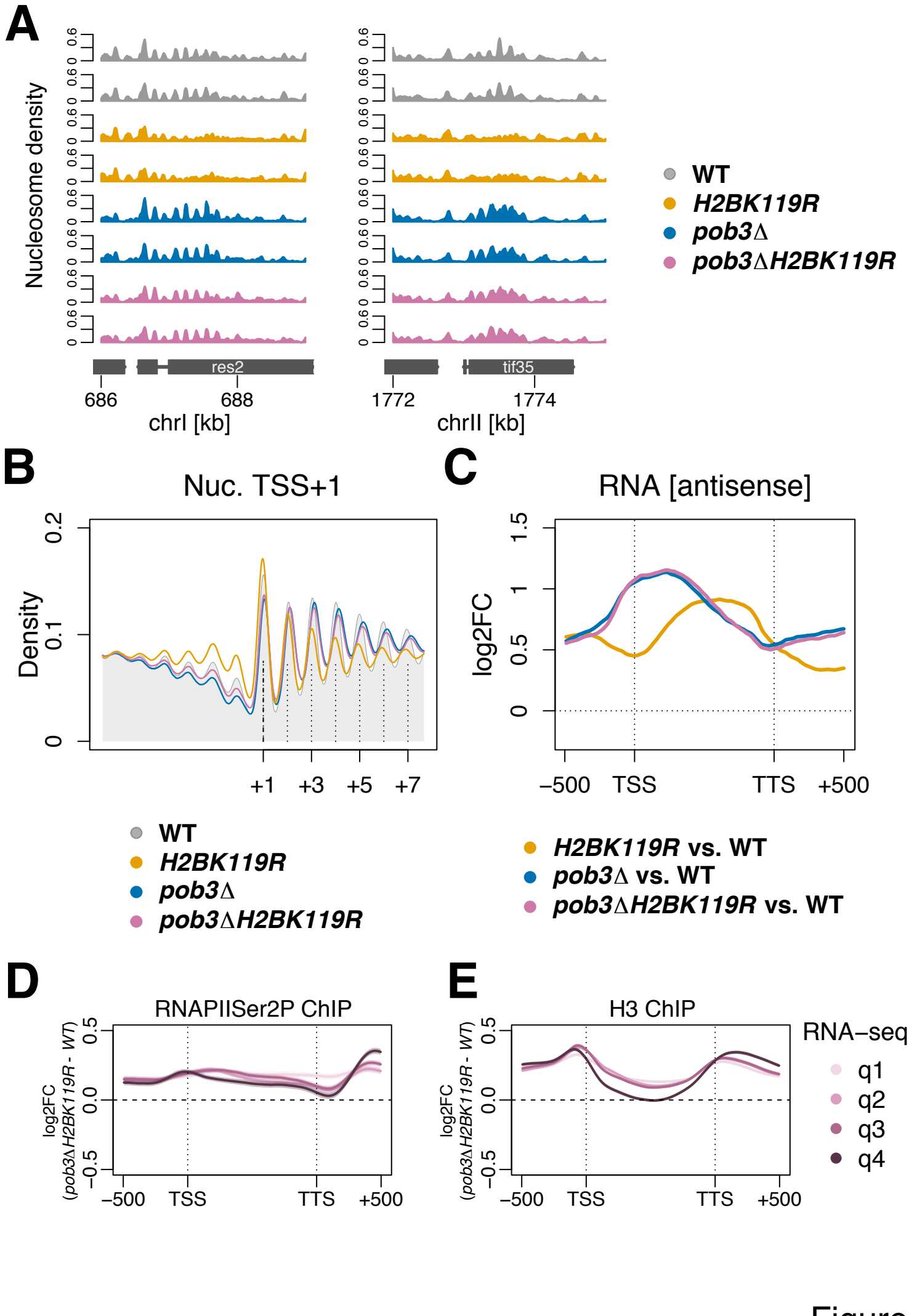

Figure 3

Figure4

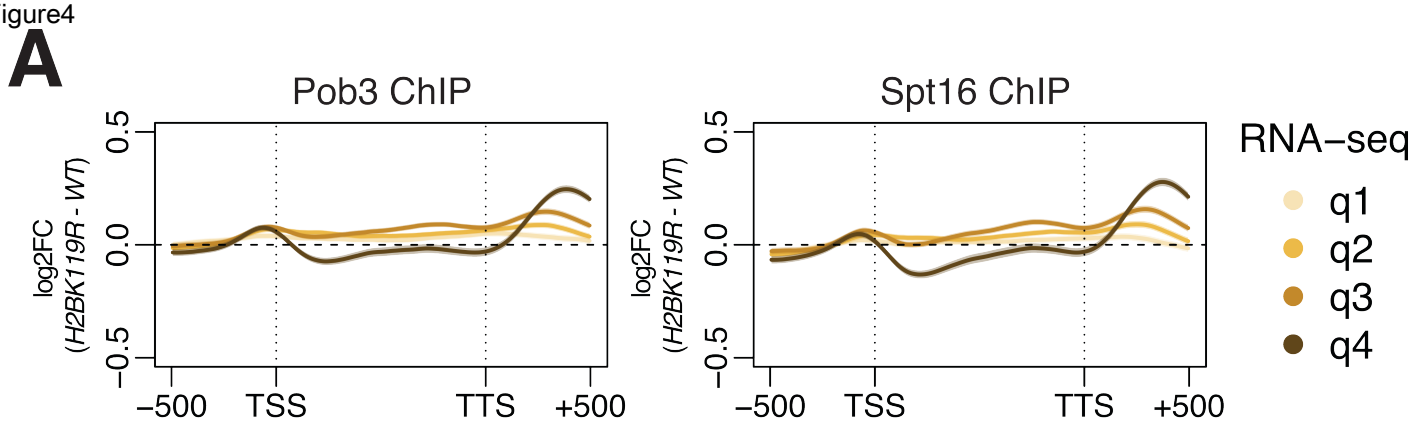

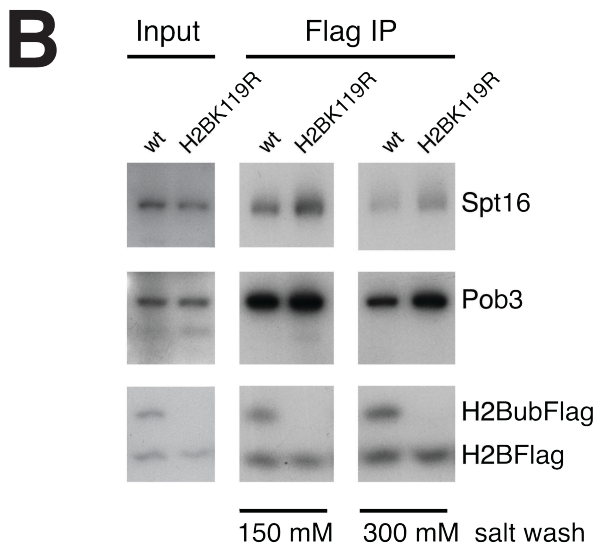

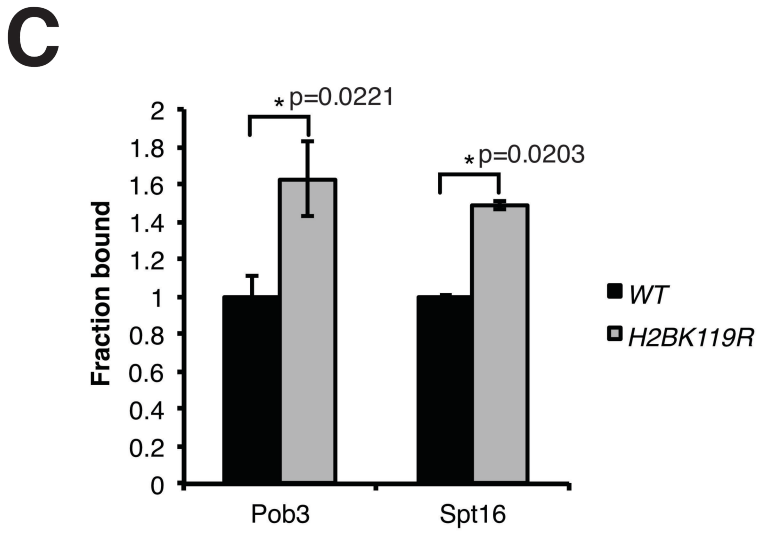

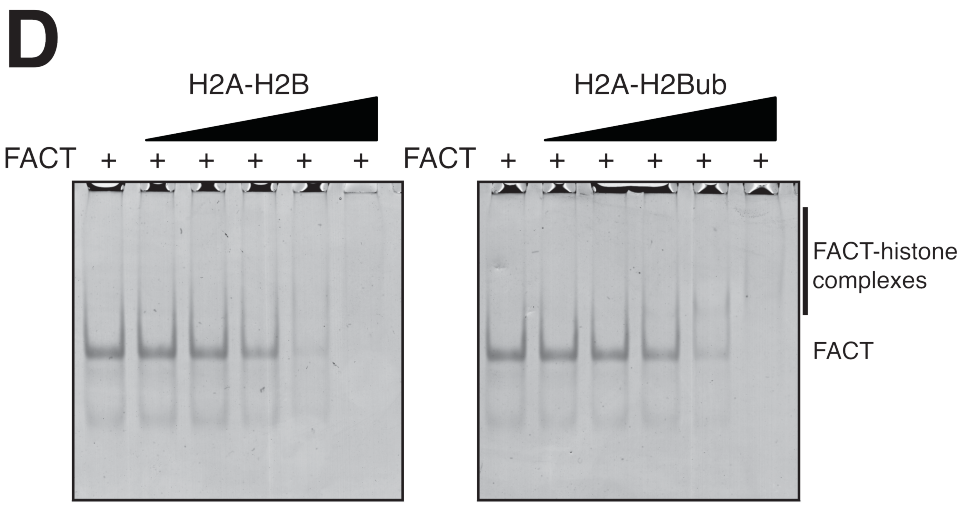

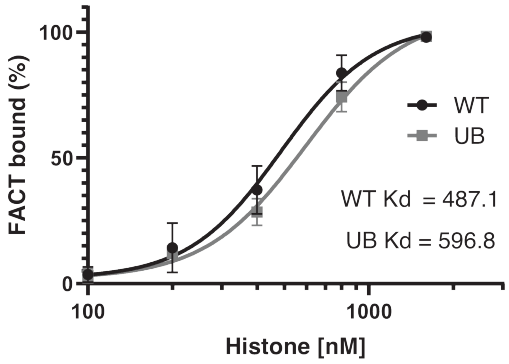

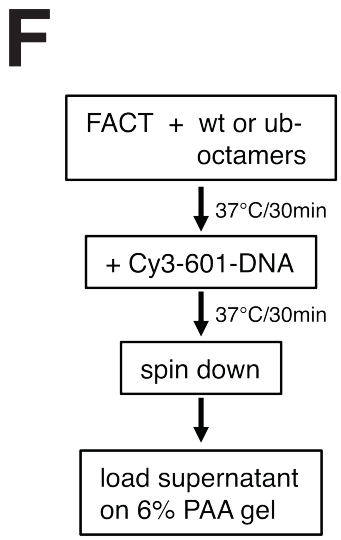

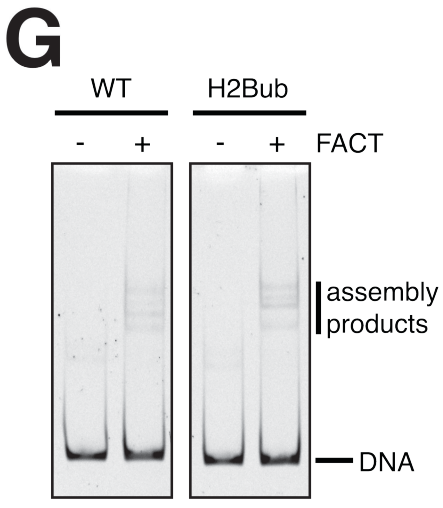

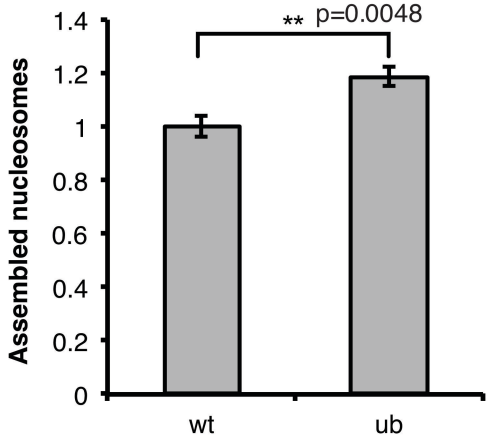

Figure 4

Figure5

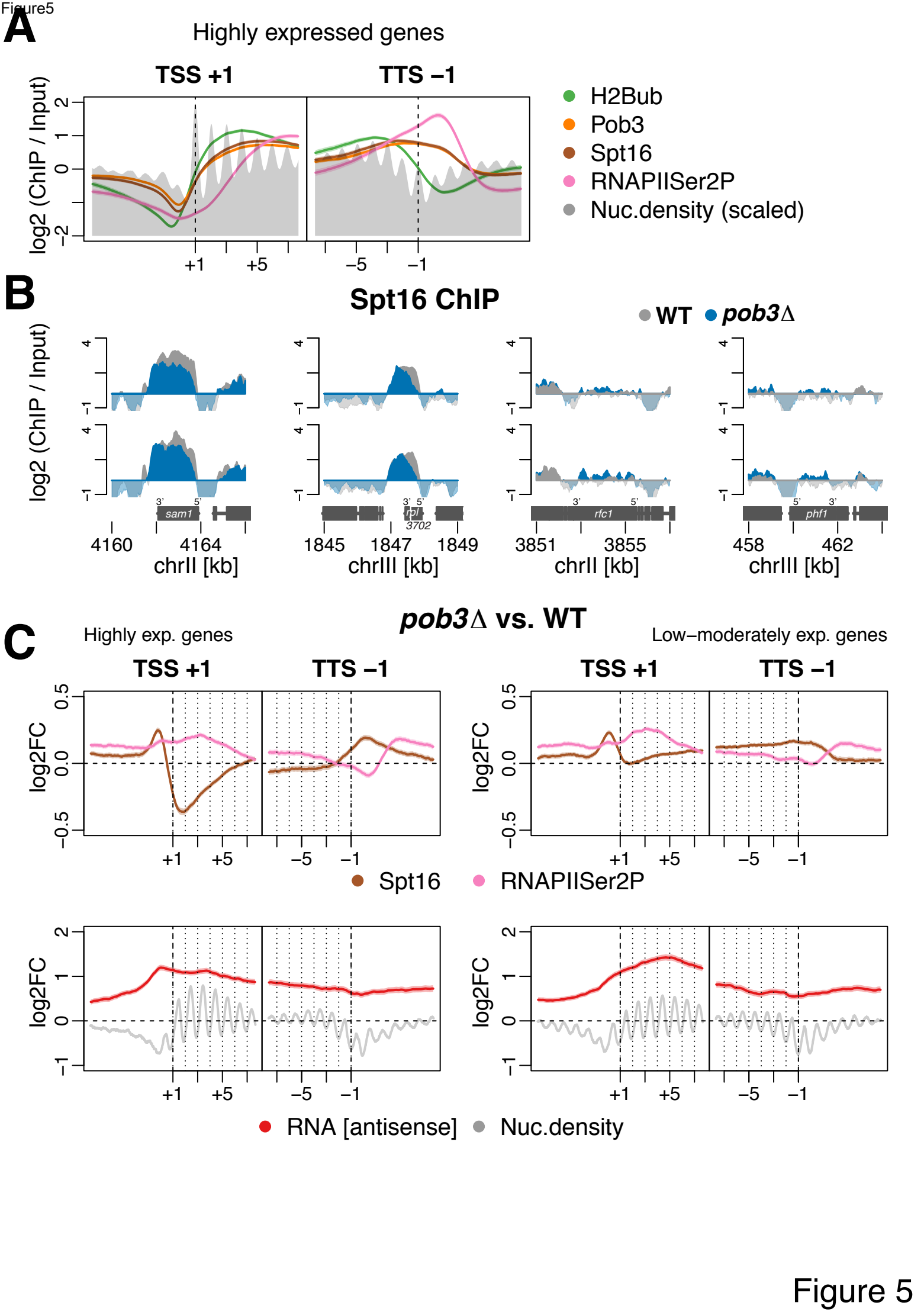

Figure 5

Figure6

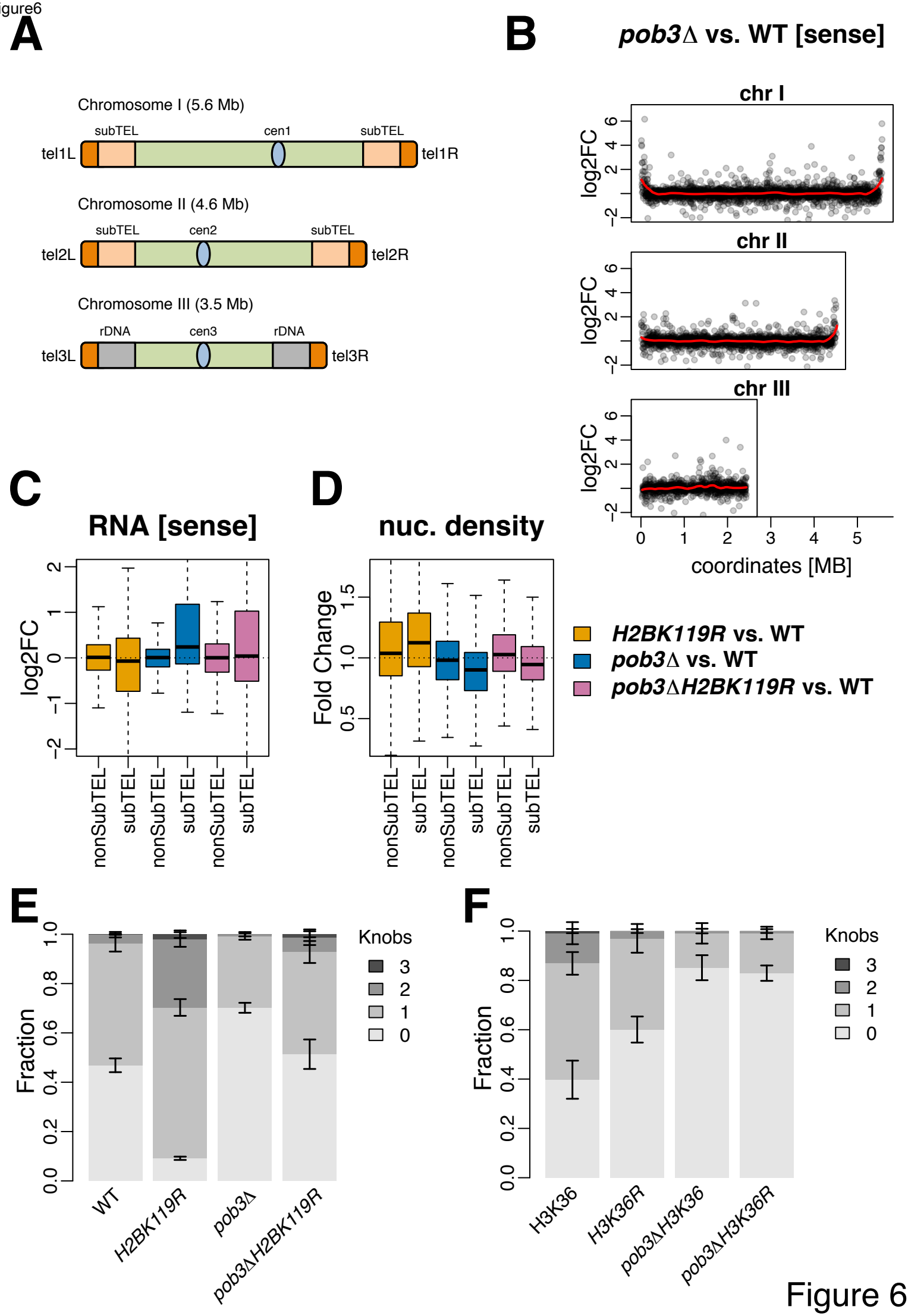

Figure 6

Figure7

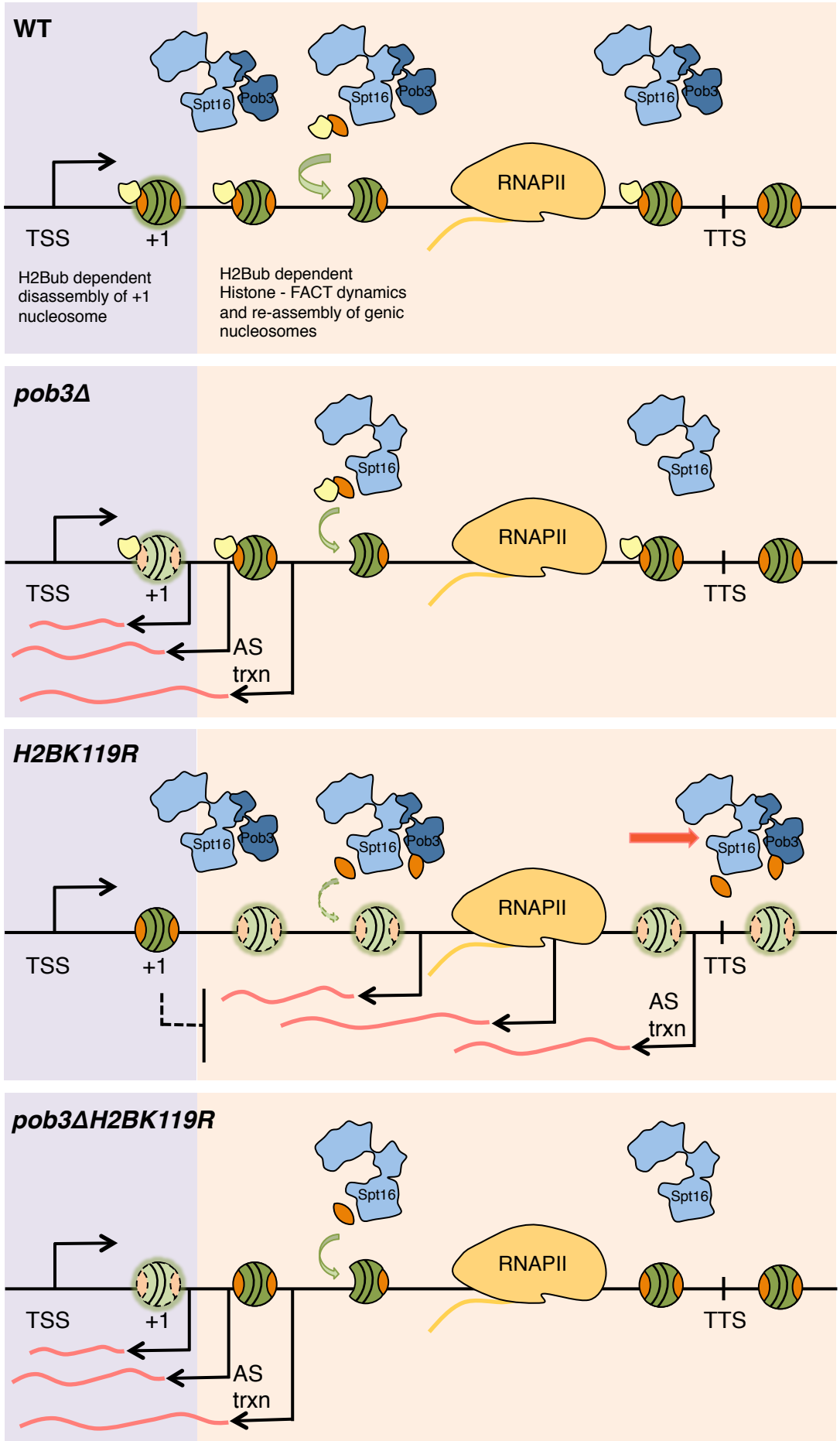

Figure 7